The Shear Behavior of Soil with Constant Structure

By

J. H. Schmertmann

University of Florida, College of Engineering, Gainesville, Florida 32611

Synopsis

This paper presents an experimental investigation of the components of mobilized soil shear resistance independent (I) and dependent (D) of effective stress when also considering strain (S) as a variable. To study the important effect of soil structure, the writer developed a test (IDS) that separates these components at approximately constant structure. Many such IDS-tests demonstrated the special and surprising behavior of the I-component in a variety of remolded and undisturbed soils. This led to the concept of the Constant Structure Mohr Envelope (CSME), the formulation of its shape in equation (6), and the experimental confirmation of equation (6). All this then led to a new method for measuring a soil's mobilized shear resistance from only internal bonds, I_0. The new method seems to produce reasonable results, has a low sensitivity to stress-dilatency effects, and permits determining I_0 as a function of strain.

This paper demonstrates that when some remolded and undisturbed cohesive soils carry load under creep strain rates they undergo soil structure modifications that transfer load to those groups of particles oriented to best resist particle dispersion. This transfer can increase dramatically the soil's mobilized shear resistance sensitivity to a change in effective stress. The transfer also leads to a temporary, with continued strain, stiffening and strengthening of the soil. Overconsolidation also produces this transfer, without significant, if any, increase in bonds. This seemingly common transfer phenomena may help to explain the important non-bond contribution to such soil behavior as "aging" and "quasi-preconsolidation" effects.

A Table of Contents is found at the end of the paper.

1. Introduction

Dr. Bjerrum always maintained a lively interest in the subject of fundamental soil shear resistance behavior. His own doctoral research, reported in NGI Bulletin No. 5, dealt with the Hvorslev effective shear strength components. In his major state-of-the-art paper to the 8th International Conference he again reviewed fundamental behavior and generously referred to the work of Hvorslev and that of myself and co-workers. In both 1951 and 1973, and in the years throughout, he attempted to draw practical implications from fundamental shear strength research and theory.

My doctorate dissertation also dealt with the Hvorslev components, and through 1971 I actively pursued research in this area. This included a 1962–63 USA National Science Foundation Fellowship under Dr. Bjerrum at the NGI. After 1963 I corresponded with Dr. Bjerrum concerning my continuing research and he contributed in a substantial way. In view of these events I look upon the invitation to participate in this volume as a very suitable opportunity to bring much of this research together in one place, to update it since the last publication in 1965, and to suggest explanations for the observed shear mobilization behavior of soils tested at constant structure.

2. The constant structure Mohr envelope (CSME)

First, consider what the term "structure" means herein. We all know that soils have an extremely complex fabric involving a three dimensional arrangement of particles, with the particles having a wide range of size, shape and mineralogy. Furthermore, there exists a complex interplay of attractive and repulsive forces between particles depending on particle spacings and orientation, the electrical and chemical activity of the particles and of natural cementing agents between particles, the age of the soil deposit, its degree of saturation, the chemical content of the pore water, etc. To permit identifying a particular state of the fabric and internal forces composing such a complex material, the writer will simply use the catch-all term of "soil structure" or just "structure".

As explained in T. W. Lambe's beautiful work (Lambe, 1953), particle dispersion represents one of the important ways in which clay structure can change. Dispersion means a more parallel, less flocculated, orientation of the platy or elongated particles typical of clay minerals. It can result from chemical additives which reduce the internal attractive forces between particles, particularly if at the edge-face contact zones. Or, dispersion can result from the mechanical strains between particles during consolidation and shear. Strain changes structure. The remolding of sensitive soils and the resulting strength

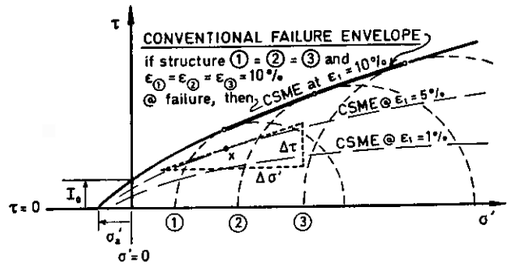

Fig. 1. Schematic illustrating when a conventional Mohr envelope also a CSME.

change can provide dramatic evidence of the mechanical strength reduction consequences of soil structure change by strain, in this case often at constant void ratio or density. C. Crawford (1963) presented photographs illustrating a striking example of such a structure change by the strains of remolding.

The reader should now imagine a soil in which changes in the level of ambient effective stress will produce only negligible changes in particle orientation, packing, etc. – therefore, negligible change in structure. Begin with an essentially identical set of isotropically consolidated soil specimens, but with each specimen rebounded to a different level of initial effective stress. Then compress each to failure in a similar manner in a conventional triaxial test machine, say with failure occurring at 10 % strain in all tests. *Fig. 1* presents the conventional Mohr-Coulomb effective stress failure envelope obtained from such a test series. Each of the three specimens began with the same soil structure and each reached the same percent at failure along the same strain path. Therefore, the writer believes they all would have the same structure at failure. For this imagined case the conventional failure envelope also represents a constant structure Mohr envelope (CSME).

Dr. E. E. de Beer (1965) expressed a similar idea and he referred to the resulting failure envelope as the "real intrinsic curve". He produced experimental intrinsic curves from tests on reassembled sands, with each test in a series beginning at the same void ratio after consolidation but before compression. Thus, he started compression with a very simple, duplicated structure, and one not sensitive to change by ambient effective stress. His "intrinsic curves" represent approximate CSMEs to the extent, unreported by de Beer, that identical void ratio and strain conditions existed at failure. Section 6.2.1 analyzes further this work by de Beer.

Consider the various envelopes also shown in the hypothetical example of *Fig. 1*, with each envelope representing the shear resistance mobilized by the soil at various, constant levels of strain less than the failure 10 %. Each of these envelopes also represents a constant-structure condition and therefore represents another CSME for the same soil.

In this paper the writer chose to work with a constant structure envelope defined in terms of the conventional shear and effective normal stress coordinates and Mohr circles determined from major and minor principle stresses, σ_1' and σ_3', only. This neglects the effect of the intermediate principle stress, σ_2'. To the extent that σ_2' has an important effect on structure, use of this set of coordinates introduces inaccuracy. The concepts developed herein might, or might not, have significantly more generality in terms of octahedral stresses.

The reader might ask why introduce a sometimes fictitious, new type of Mohr envelope? The reason – to investigate strength fundamentals without the serious complicating effects of varying soil structure. The slope of the CSME at any point, such as x in *Fig. 1*, represents the shear resistance mobilization sensitivity of that particular structure to a change in the level of effective stress. Furthermore, if the structure remains constant along such an envelope, then strength components such as real cohesion, or the alternate term "bond shear strength" used herein, remain constant. Then the intercept of the CSME with the $\sigma' = 0$ line, denoted I_0 in *Fig. 1*, represents the real mobilized bond shear resistance of that structure. The intercept with the $\tau = 0$ axis represents the mobilized effective tension resistance of that structure, σ_a'. The slope at any point, $\Delta\tau/\Delta\sigma'$; expresses the sensitivity of that structure's shear mobilization to a change in effective stress. An investigator can obtain these more fundamental strength properties of a given soil structure from a CSME. He cannot from conventional Mohr envelopes, even in the form of constant strain contours, because volumetric strain, and therefore structure, usually varies very significantly at different levels of effective stress along conventional envelopes.

At this point the reader has only the de Beer tests on sands as evidence of the possible real existence of such CSME's. De Beer approximated the CSME condition at failure and drew some important, more fundamental conclusions – especially with respect to the curvature of such an envelope. However, Professor P. Rowe, by use of his famous stress-dilatency theory, also produces no-structure, and therefore a special case of constant structure, envelopes mathematically via a structure-dilatency correction. He thus eliminates the effects of different structure along a Mohr envelope and produces a no-dilatency CSME. Use of this no-dilatency CSME has permitted measuring some of the more fundamental soil shear strength properties. The writer attempted to construct parts of CSMEs and then reason the behavior of complete CSMEs. He also eventually produced complete CSMEs by means of the experiments and their mathematical interpretation as described subsequently.

3. The IDS-test

3.1 GENERALIZING THE HVORSLEV COMPONENTS

Starting in 1958, the writer began an experimental investigation aimed at determining the Hvorslev effective shear strength components as functions of strain. However, as explained in detail by Schmertmann & Osterberg (1961b),

and Schmertmann (1962a), these components, as originally defined by Hvorslev, prohibited any determination as functions of strain. The Hvorslev components first required a slight modification and a resultant generalization, as explained by Schmertmann (1963a). This modification included a slight relaxation of the Hvorslev requirement of exactly the same void ratio for soil specimens to have equal cohesion, in favor of a definition that permitted small, seemingly negligible, differences in void ratio in favor of much better assurance of equal structure.

The problem required an experimental technique that would test a soil structure, subject to modification by strain, at two levels of effective stress. The change in mobilized shear resistance with a change in effective stress then would indicate that structure's sensitivity to such a change, and therefore presumably measure its friction behavior. Extrapolating this change to $\sigma' = 0$ would presumably produce the cohesion intercept. At first the writer denoted the test designed to accomplish the separation of Cohesion and Friction as functions of Strain as the CSF-test. Later, as explained subsequently, the writer realized that CSME curvature prevented these components from being fundamental friction and cohesion and changed the test notation to the IDS-test. "*I*" denotes that component seemingly independent of effective stress change and "*D*" that component seemingly linearly dependent on effective stress change. The following presents an outline of the history and details of the performance of IDS-tests.

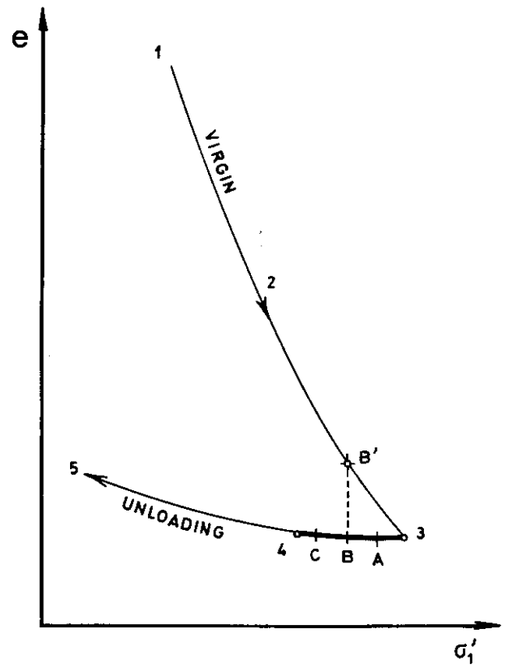

Fig. 2. Use early part of effective stress unloading for best constant-structure conditions.

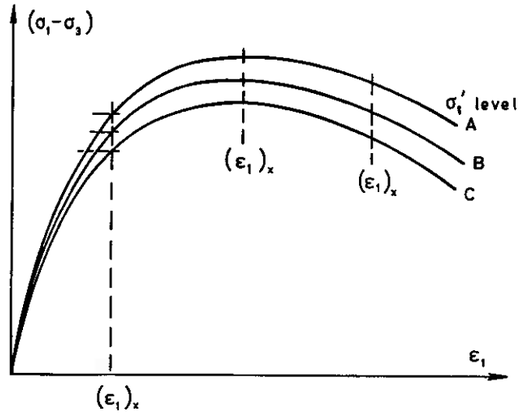

Fig. 3. Schematic of different shear mobilization with strain at the A, B, C effective stress levels in Fig. 2.

3.2 TEST DEVELOPMENT TO THE USE OF A SINGLE SPECIMEN

Consider a soil subjected to initial, or virgin, compression followed by simple unloading. *Fig. 2* illustrates that a unit change in effective stress during initial compression produces a much greater change in void ratio, and presumably structure, than similar change during unloading. If one desires to change effective stress with a minimum of change in structure, one should confine effective stress changes to the rebound region designated by 3–4 in *Fig. 2*.

Imagine three initially identical specimens consolidated to point 3 in *Fig. 2*. Then allow one to rebound to σ_1' at point "A", another point "B" and third to point "C". Although each reaches a progressively reduced effective stress, all other aspects of structure should remain almost the same. Further imagine each of these almost identical specimens then subjected to similar compression tests in such a way that σ_1' never exceeds point 3 in *Fig. 2*. *Fig. 3* illustrates results qualitatively typical of many experiments. Because specimen A has a greater effective stress at all strains than B, and B greater than C, the soil structure at A can mobilize greater shear resistance than B at all strain, and B greater than C. At any strain $(\varepsilon_1)_x$, either before, at, or after any definition of failure, the mobilized resistances of specimens A, B and C can be represented by three Mohr circles all applicable to that soil at $(\varepsilon_1)_x$. *Fig. 4* illustrates such circles. The envelope defined by these circles, represents a piece of the CSME that applies to the soil shown in *Fig. 2* after shear mobilization to strain $(\varepsilon_1)_x$ in *Fig. 3*.

The slope of this piece of the CSME expresses the shear resistance sensitivity of that constant structure to a probing change in effective stress – a change sufficient to cause a measurable change in shear resistance but not sufficient to produce a significant change in soil structure. Note the slope $\Delta\tau/\Delta\sigma_t' = d_e$, and $D = \bar{\sigma}_t' d_e$.

As shown by Schmertmann & Osterberg (1961b) any piece, such as x–y, of a CSME appeared linear in their

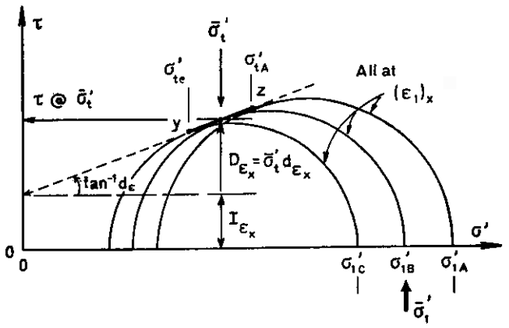

Fig. 4. The piece-CSME construction to determine the I and D components at any strain in Fig. 3.

pioneering IDS-test work. A linear extrapolation to the $\sigma' = 0$ axis produced an intercept denoted as the I_ε-component, considered that component of mobilized shear resistance, at strain ε, seemingly independent of effective stress. The remaining component indicated in *Fig. 4*, D_ε, represented that component at ε seemingly linearly dependent on effective stress. The two components I_ε and D_ε, or just I and D for convenience, apply only to the particular structure under consideration at strain ε. Hence the designation IDS-test. An investigator could make a similar component determination to that shown in *Fig. 4* at any strain in *Fig. 3*. Plotting the results of such component determinations vs. strain then permits the further determination of the variation of these components as functions of strain, thus reaching the desired objective. *Fig. 5* illustrates such a determination typical of those obtained from triaxial compression tests on remolded clay.

The techniques used to perform an IDS-test started with multiple-specimen tests such as illustrated in *Fig. 3*. However, a succession of refinements proved it possible to achieve very similar, and perhaps superior, results using only a single specimen. Instead of developing the three or more Mohr circles shown in *Fig. 4* for the component separation at a given structure, the apparent linearity of small pieces of the CSME suggested only two circles as sufficient. This reduced to only two the number of comparative stress strain curves in *Fig. 3*. Furthermore, instead of requiring two initially duplicate specimens, such as A and C, experiments showed (Schmertmann, 1962b) that one could obtain very similar results from a single specimen by hopping back and forth between the A and C effective stress conditions during the progress of strain in a strain controlled compression test. This one specimen test has the great advantage of not requiring initially, always questionable, duplicate test specimens. This gave further assurance that the A, B, and C curves in *Fig. 3*, or just A and C, had nearly identical structure at any given strain. It also permitted testing undisturbed soils or soils from which it might otherwise prove difficult or impossible to obtain duplicate specimens.

3.3 VARIETY OF IDS-TESTS

It also proved possible and sometimes useful to perform IDS-tests of different types. At first the writer performed only tests where each of the curves in *Fig. 3* represented stress-strain mobilization at a constant σ_1'. The purpose of the constant-σ_1' form of the test was to better assure that major structural changes would not take place in the soil during strain as a result of σ_1' exceeding the preconsolidation σ_1' at point 3 in *Fig. 2*. But, maintaining constant-σ_1' required continuous adjustment of pore pressure during the strain. In principle any type of test that develops the *Fig. 3* curves between two or more different levels of effective stress will provide the data for the required Mohr circle separations at constant structure in *Fig. 4*. Experience has shown that curves similar to A and C would also result from IDS-tests at constant-σ'_{oct}, constant-σ_3', or two levels of constant volume. For the constant-volume IDS-tests the investigator controls volume between two pre-selected levels and has to measure pore pressures to obtain the effective stress differences between curves A and C – see Schmertmann (1963a, p. 265) for an example.

Furthermore, the investigator need not restrict the IDS-test to the triaxial compression test at controlled strain rate. In principle he or she can perform an IDS-test with any shear testing equipment capable of generating stress-strain curves with a controlled difference in effective stress conditions. For example Schmertmann (1963b) performed IDS-tests (the "X" points in Fig. 11 i) with strain controlled, direct, simple shear equipment. Topshøj (1970) performed the IDS-tests using axial extension and produced results testing kaolinite similar to those from axial compression tests. The IDS-test can also be performed using stress-control methods and two specimens, as shown by Schmertmann (1963a, pp. 267–268).

4. The constant I-component

Altogether, the writer has performed, or supervised the performance of, about 500 IDS-tests at the University of Florida. These tests produced much information about the I and D components and their possible significance. This paper can only summarize some of these results. One of the most important discoveries concerned the remarkable and unexpected behavior of the I-component. As explained previously, the I-component represents a cohesion-related concept. The D-component seems friction-related. The fundamental work of Hvorslev suggested that any effective or "true" cohesion, and therefore presumably also the I-component, should vary with the variables of void ratio, the degree of dispersion or flocculation of the soil structure, the nature of the soil pore fluid, previous stress history effects such as overconsolidation, clay mineralogy, etc. But, I, as measured by its maximum value I_m (see *Fig. 5*), proved essentially independent of all of these variables. The following summarizes much of the data leading to this strange conclusion.

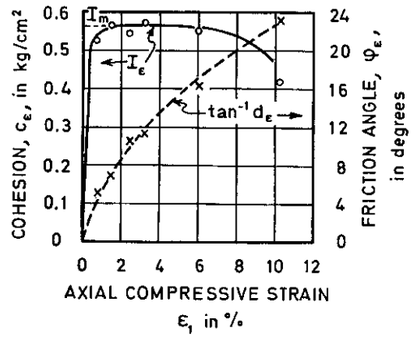

Fig. 5. Example of the determination of the I and D components as functions of strain.

4.1 THE CONSTANCY OF I_m

4.1.1 *Particle dispersion*

Table 1 presents a comparison of I_m from remolded kaolinite and Boston blue clay, before and after the addition of trace amounts of sodium phosphate dispersants. Judging by the large change in *PI*, the reduction in shrinkage limit (SL), and the large reduction in equilibrium void ratio at the constant effective stress conditions for all tests compared, the phosphates produced dramatic changes in structure. Yet, I_m remains virtually constant. Note that unless otherwise designated, the IDS-tests which produced these and subsequent data were of the constant-σ_1' type.

4.1.2 *Void ratio and overconsolidation*

In 1960 Dr. J. Hall (then a graduate student) and the writer performed a most informative series of IDS-tests using a large number of saturated, machine extruded specimens with initial structure virtually identical. We then subjected these specimens to various levels of normal and overconsolidation, after which we subjected them to a constant-σ_1' IDS-test. *Fig. 6* presents the results obtained, showing both void ratio changes during consolidation and during the IDS-test itself, and I_m vs. $\bar{\sigma}_1'$. The writer performed the first series of tests, shown with solid symbols, and Dr. Hall performed the second (open symbols) over the summer of 1960 when the writer was absent. These two separate sets of data matched very well, and show clearly that I_m is virtually independent of final void ratio and instead depends linearly on the average value of σ_1' actually used during the one-specimen test curve-hopping procedure described in 3.2. *Fig. 4* also illustrates the meaning of the average σ_1' value, $= \bar{\sigma}_1'$.

We also performed a similar series of tests on a natural but remolded clay (Enid) with very different grain size distribution and mineralogy, and obtained very similar results.

The tentative conclusion was both surprising and inescapable – I_m did not vary with the great void ratio changes, and presumably great structural changes, associated with virgin consolidation followed by rebound, provided one compared I_m using the same $\bar{\sigma}_1'$.

4.1.3 *Simple overconsolidation*

Consider two points at the same σ_1', such as B and B′ in *Fig. 2*, one normally consolidated (B′) and one overconsolidated (B). They both have the same effective stress but certainly different structure as a result of the void ratio reduction associated with overconsolidation. For example, test numbers 108 and 112 in *Fig. 6* have a B–B′ relationship. *Fig. 7(a)* presents the IDS-test stress-strain curves obtained from tests 108 and 112, and also the subsequent check test H-45. *Fig. 7(b)* shows the resultant I-components as a function of strain. Note that I, as well as I_m, stays about the same, and perhaps even *decreases* somewhat as a result of the overconsolidation. In great contrast, *Fig. 7(b)* shows a dramatic increase in the strain-rate mobilization of the D-component, illustrated here via d_ε. As a further example of this important discovery, *Fig. 8(a)* and *8(b)* show the same comparison for a remolded natural clay (Enid) with different mineralogy. To date we found this behavior in all soils tested. Clearly, the structure changes associated with overconsolidation had little if any effect on the I-component, but did dramatically affect the D-component.

4.1.4 *Primary and secondary consolidation time effects*

As also indicated by the notes in *Fig. 6*, varying the length of time allowed for the completion of primary consolidation from 24 to 120 hours, or whether or not an intermediate complete unloading occurred, had little

Table 1. I_m vs. structure at $\bar{\sigma}_1' = 2.95$ kg/cm².

Clay	Abbrev.	Shrinkage limit (*SL*)	*PI*	Void ratio	I_m (kg/cm²)	Structural condition
Kaolinite	DWEPK	25.0	21	0.888	0.54	Extruded, no chemical dispersion
Kaolinite	N-EPK	21.9	8	0.783	0.50	$Na_2HPO_47H_2O$ dispersed
Kaolinite	DWEPK		21	0.898	0.57	Extruded, no chemical dispersion
Kaolinite	Q-EPK	19.2	4	0.674	0.56	$Na_6P_4O_{13}$ dispersed
Boston Blue clay	BBC		19	0.659	0.50	Extruded, no chemical dispersion
Boston Blue clay	BBC		19	0.648	0.46	Extruded, no chemical dispersion
Boston Blue clay	Q-BBC		11	0.532	0.49	$Na_6P_4O_{13}$ dispersed

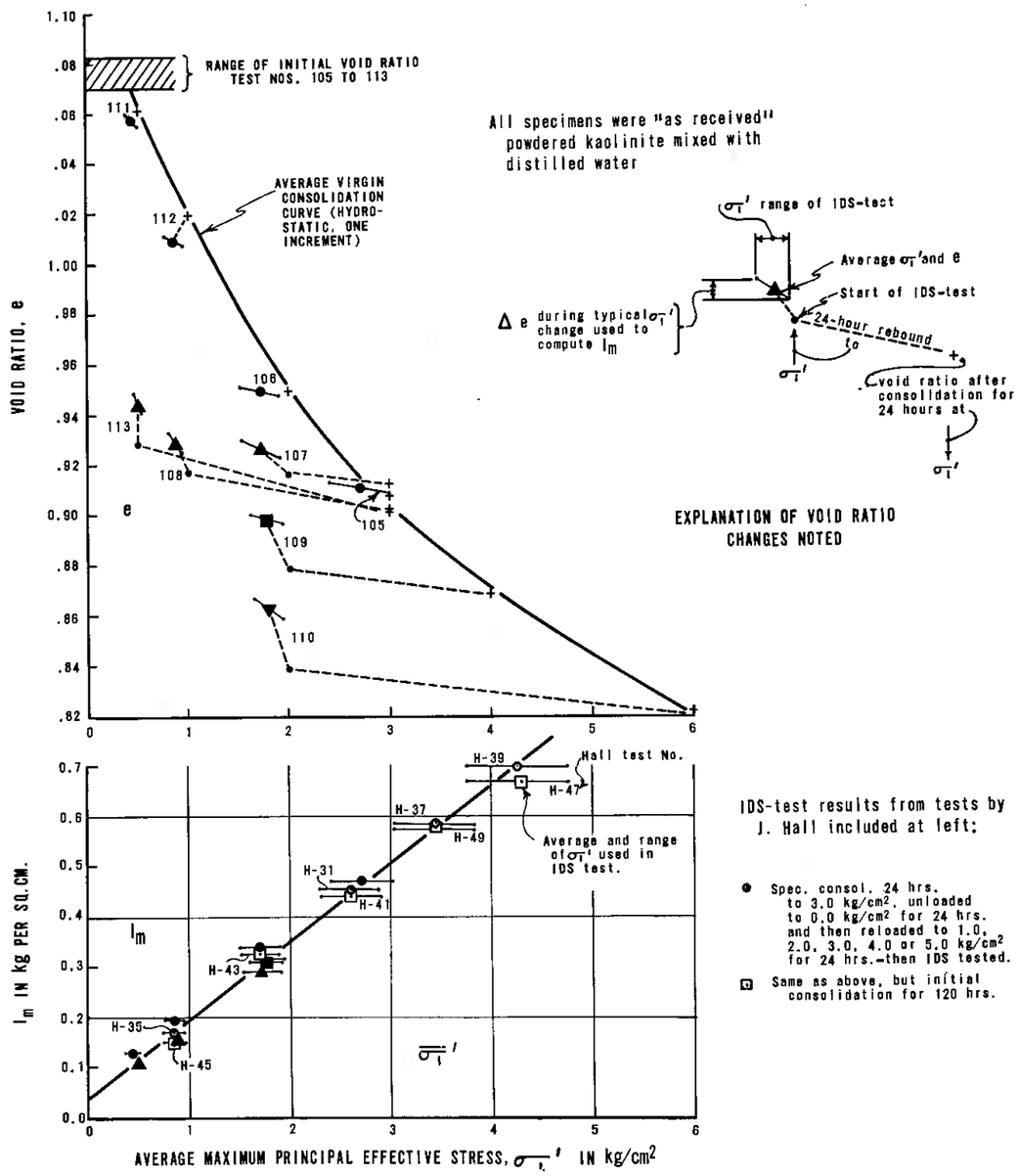

Fig. 6. Demonstration that I_m independent of void ratio and simple laboratory overconsolidation in extruded, distilled water kaolinite (DWEPK).

or no effect on the constant-σ_1' IDS-test values of I_m. The writer investigated further the effect of different primary times on the I_m value in remolded kaolinite and Enid clays by providing progressively more internal and external drainage aids to speed consolidation. *Table 2* presents the results and shows that changing the primary time by a factor of 10 appeared to have no effect on I_m.

The writer also tried various combinations of sudden loading and constant-rate loading to produce the consolidation, various times in secondary followed by unloading and reloading, etc. as explained briefly in *Table 3*. In all cases consolidation ended with a normally consolidated clay at the same final effective stress and produced the same I_m. It seemed clear that the method of primary consolidation had no effect on I_m.

The effects of allowing progressively increasing times for secondary compression (under constant effective stress conditions) proved informative. *Fig. 9* shows the

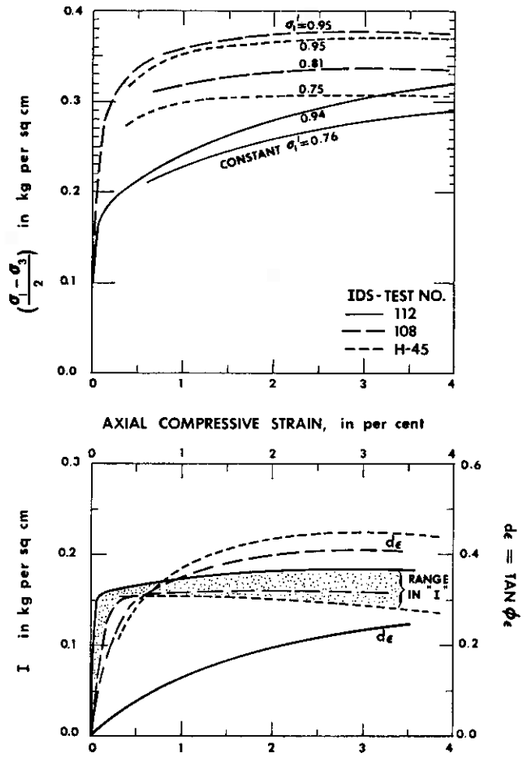

Fig. 7. Comparisons of shear component mobilization in NC and OC (R = 3) extruded kaolinite clay.

IDS-test components obtained from a comparative series, again on remolded kaolinite, with all other test conditions the same. Note again that I_m remains about the same (differences in strain-mobilization probably mostly experimental variations). Again in contrast, there occurs a dramatic increase in the strain-rate of d_ε mobilization, especially at low strains. Compare with *Figs 7* and *8* and it appears that secondary compression has much the same effects, at least at low strain, as simple overconsolidation. Similarly, the structural change effects of longer secondary compression times produced, as with overconsolidation, structural changes which greatly affected d_ε but did not affect I_m.

Table 2. I_m vs. time for primary consolidation.

Clay	Primary time (Min.)	I_m (kg/cm²)
Kaolinite	22	0.57
Kaolinite	34	0.57
Kaolinite	60	0.56
Kaolinite	100	0.53
Kaolinite	250	0.56
Enid	25	0.52
Enid	55	0.52
Enid	80	0.54

Consider the nature of the structural change that increases d_ε. *Fig. 9* also shows via a heavy solid line the low-strain part of the d_ε-strain mobilization curve from a constant-σ_1' IDS-test on deliberately dispersed kaolinite (by $Na_6P_4O_{13}$), Q-EPK, prior to specimen extrusion. As discussed in 4.1.1, and shown in *Table 1*, the addition of this dispersant did produce a dramatic dispersion of structure (destroys edge-face particle contacts and forms a more parallel particle arrangement).

Note the heavy line matches almost exactly the d_ε mobilization of the distilled water kaolinite after a 5-week secondary. This suggests that the structure change during secondary may be closely related to dispersion. Overconsolidation increases particle orientation and therefore disperses structure. The similar effect of secondary on d_ε supports the dispersion hypothesis. The writer discusses further this important hypothesis in Sections 10.5 and 10.9.

4.1.5 *Anisotropic consolidation*

In an extensive series of tests with remolded kaolinite and Boston blue clays reported in detail by Schmertmann and Hall (1961a), the authors showed (see examples in *Figs 23(a)* and *23(b)* that the mobilization of the I-component

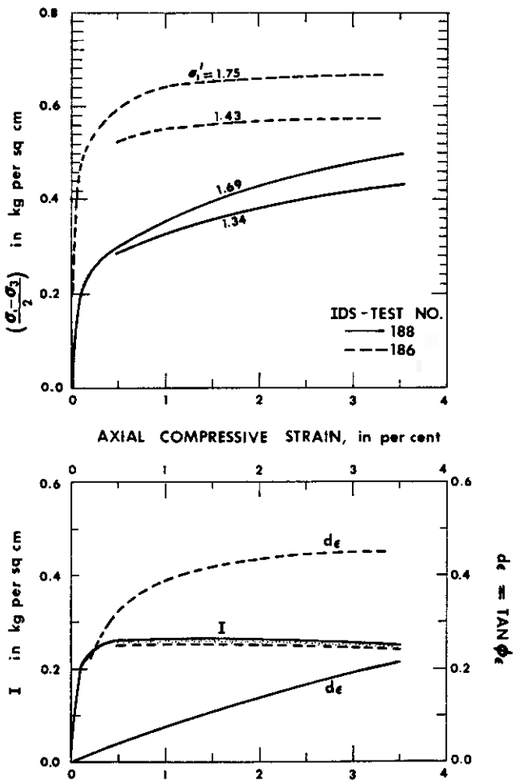

Fig. 8. Comparisons of shear component mobilization in NC and OC (R = 4) extruded Enid clay.

Table 3. I_m vs. method for hydrostatic consolidation. (All tests at approximately $\sigma_1'_h = 3.30$ and $\sigma_1'_l = 2.60$ kg/cm²).

Clay	Methods of consolidation	I_m (kg/cm²)
Extruded Kaolinite	6 days in "secondary", but without drainage, then immediate IDS-test	0.56
Extruded Kaolinite	6 days in secondary at $\sigma_c' = 0.50$ after consolidation to 3.50, then returned to $\sigma_c' = 3.50$ for 1 day	0.57
Extruded Kaolinite	7 days at $\sigma_c' = 3.50$; then held at 0.20 for 8 days; then returned to 3.50 for ½ day	0.57
Extruded Kaolinite	Consolidated to $\sigma_c' = 3.50$ for 1 day and tested, both with back pressure of 3.00	0.55
Extruded Kaolinite	Consolidated to $\sigma_c' = 3.50$ with constant rate of loading for 10 days; then held at 3.50 for one day	0.63
Extruded Enid	Consolidated to $\sigma_c' = 3.50$ with constant rate of loading for 10 days; then held at 3.50 for one day	0.59

during the IDS-test following anisotropic consolidation to various K' values, including K_0', did not change the I-component with subsequent compressive strain. Once again, the D- (or d_ε) component changed dramatically by increasing as K' decreased. Note that in this reference

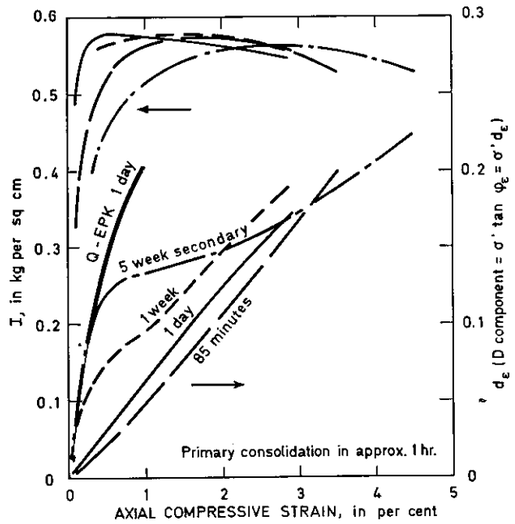

Fig. 9. Effect of secondary isotropic consolidation times on I and D in extruded kaolinite clay.

$c_\varepsilon = I_\varepsilon$ and tan $\varphi_\varepsilon = d_\varepsilon$. Once again, the soil structure differences associated with different levels of K' consolidation did not produce changes in I_m.

4.1.6 *Clay mineralogy and grain size*

Table 4 a presents a list of the I_m values obtained from constant-σ_1' IDS-tests on remolded clays with a variety of mineralogy and plasticity. Despite the *PI* varying from 4 to 105 % and clay minerals from kaolinite to montmorillonite, the average I_m values at the same σ_1' test levels vary from only 0.47 to 0.62, with most around the average 0.55 kg/cm². Again the writer concluded that the likely major differences in soil structure associated with these major differences in clay mineralogy have only a minor effect on I_m.

However, not all soils will produce the same I_m at the same effective stress levels. For example, consider the non-plastic quartz soils listed in supplemental *Table 4 b*. One might expect that non-plastic soils would not have a cohesion-related I-component intercept. This proved untrue as shown in *Table 4 b*. However, the writer observed a definite trend of reducing I_m with increase in grain size at the same effective stress, and will return to this important point in subsequent Section 10.

4.1.7 *Rate-of-strain effect*

Schmertmann and Hall in their closure (1962) presented data from a 7-test series of constant-σ_1' IDS-tests on

Table 4 a. Data indicating I_m approximately independent of clay mineralogy at constant effective stress.*

Remolded clay	*PI* %	<0.002 mm %	Activity	Clay minerals	I_m (kg/cm²) Range	I_m (kg/cm²) Av.
Dispersed kaolinite (Q-EPK)	4	60	0.07	Kaolinite – 99 %	0.55–0.57	0.56
Enid (residual)	9	20	0.45	Kaolinite – 15 % Illite – 10 %	0.50–0.55	0.53
Jacksonville	14	13	1.08	Montmorillonite – 10 %	0.53–0.57	0.55
Boston blue	19	53	0.36	Illite – 45 % Chlorite – 25 %		0.47
Kaolinite	21	60	0.35	Kaolinite – 99 %	0.53–0.57	0.55
Lake Wauberg	105	85	1.24	Montmorillonite – 85 % Illite – 5 %		0.62

* All I_m results from constant-σ_1' IDS-tests using:
isotropic consolidation to 3.50 kg/cm²
$\sigma_1'_{high} = 3.30$ kg/cm²
$\sigma_1'_{low} = 2.60$ kg/cm²

Table 4 b. Supplemental data from non-plastic soils.

Soil	*PI* %	D_{50} mm	Mineral	I_m (kg/cm²) av.
Crushed quartz	0	0.007	Quartz	0.40
Beach sand	0	0.14	Quartz	0.22
Ottawa sand	0	0.8	Quartz	0.08

kaolinite in which they varied the constant rate- of-strain by a factor of over 5000. They showed, at least for this clay, that rate-of-strain did not significantly affect the I_m value. However, reducing the rate-of-strain did significantly increase the strain-rate of d_ε mobilization. Once again, any structural changes from this variable appeared to affect the D-component and not the I-component.

4.1.8 *Type of pore fluid*

In 1962 the writer performed a test series involving only 5 constant-σ_1' IDS-tests with kaolinite saturated by water and other fluids. The same kaolinite powder used previously in saturated, extruded kaolinite specimens was here first compacted into a mold while still hot from drying in the oven. A vacuum was then applied to the top of the specimen and fluid allowed to come in from the bottom until near-saturated. All specimens were then consolidated isotropically to 3.50 kg/cm² and IDS-tested using curve hopping between the constant-σ_1' values of 3.30 and 2.60 kg/cm² and using the same compressive strain rate for each of the 5 tests. *Table 5* presents supplementary data on the pore fluids used, etc. Despite the dramatic difference in dielectric and viscosity properties of these fluids, they all produced about the same I-components, as shown in *Fig. 10*. However, once again the d_ε component varied dramatically with the pore fluid and most dramatically with its viscosity.

As also shown in *Fig. 10*, I_m increased from about 0.55 kg/cm² for the water-saturated extruded kaolinite, compared to about 0.75 kg/cm² for the specimens first compacted dry and then saturated. Although the dry material had a higher void ratio, presumably it also had a greater number of solid-solid contact points which somehow

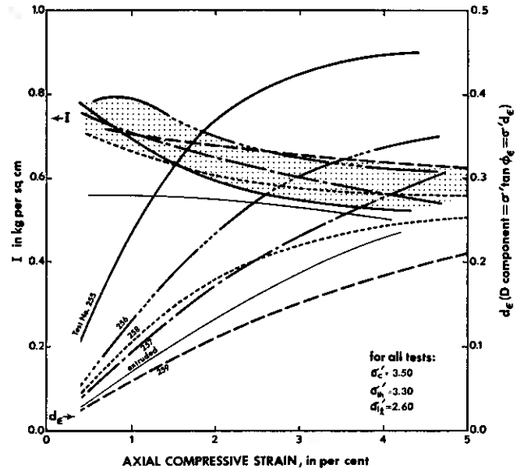

Fig. 10. Effect of different pore fluids on *I* and *D* mobilization in compacted dry, then saturated, kaolinite powder (see Table 5).

increased I and I_m. This difference in I decreased with increasing strain past I_m.

4.2 I_m NOT COHESION

All, or at least many, of the variables discussed in 4.1 should have had a dramatic effect on any true soil cohesion, assuming such cohesion due to the interplay of particle geometry and attractive and repulsive forces between particles – particularly at or near the zones of closest particle approach or contact. Yet, I_m and *I* appear independent of these variables. The conclusion seems inescapable that the I-component cannot represent true soil cohesion in the sense that soil engineers ordinarily imagine it. However, the $\sigma_t' = 0$ axis intercept must include any true cohesion. Either true cohesion has a much different origin and behavior than visualized or *I*, and I_m, result primarily from other effects. Perhaps true cohesion represents such a small part of I_m that significant changes in such cohesion from changes in the 4.1 variables does not change I_m sufficiently to detect easily. The writer believes this "minor-part-of-I" explanation.

Table 5. Test conditions for constant-σ_1' IDS-tests using kaolinite saturated with different pore fluids (match with Fig. 10).

Test No.	Pore fluid	Bulk properties: Viscosity (cp)	Bulk properties: Dielectric constant	Bulk properties: Specific gravity	Computed void ratios: As compacted	Computed void ratios: After consolid.	Computed void ratios: After IDS-test	Final degree of saturation	Time for primary consol. (min.)
255	Dry nitrogen	0.02	1	0.001	1.417	1.341	1.239	0.7	inst.
256	Benzene	0.65	2	0.899	1.416	1.292	1.202	95.9	7
257	Methyl alcohol	0.59	31	0.810	1.392	1.261	1.057	97.6	40
258	Distilled water	1.00	81	0.998	1.341	1.060	0.981	97.3	150
259	25 % glycerine 75 % distilled water	2.10	75	1.065	1.447	1.010	0.972	97.8	230
Av. of three	Distilled water*				1.028	0.895	0.898	99.9	70

* Specimens machine extruded in saturated condition.

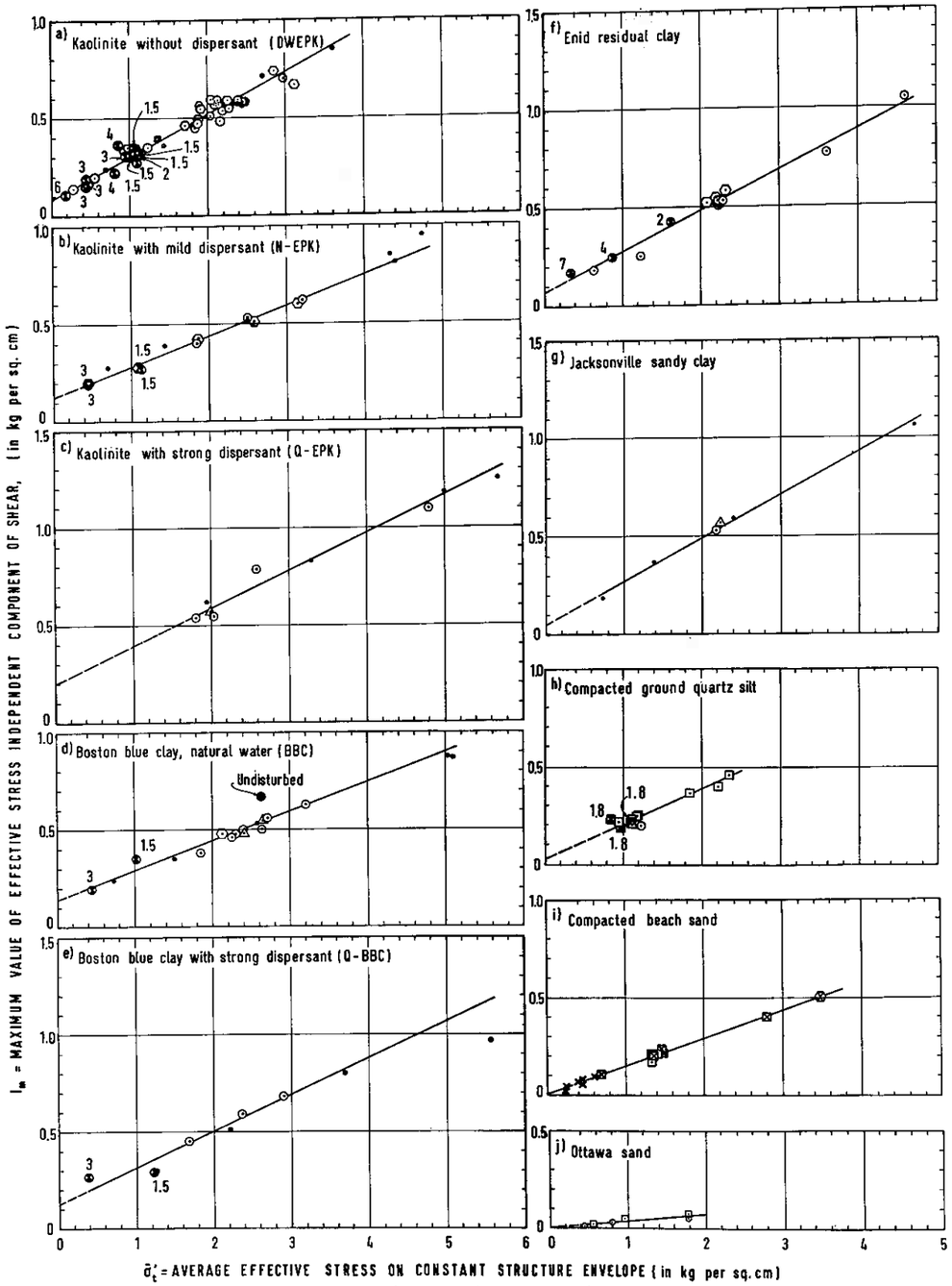

Fig. 11. Examples of the linearity of I_m vs. σ_t' in remolded soils.

5. I-component linear with effective stress

5.1 CONSIDERING I_m

The reader probably noted in *Fig. 6* that I_m varies linearly with the average of the two constant σ_1' levels of curve hopping in these constant-σ_1' IDS-tests. This behavior produced a paradox! The I-component represents that portion of the mobilized shear resistance of a soil that appears, after linear extrapolation, to be independent of the level of effective stress (see *Fig. 4*). Yet, this supposedly effective-stress-independent component itself varies linearly with the level of effective stress!

The writer then tested a variety of cohesive and cohesionless soils to examine the possible generality of this linear behavior. *Fig. 11*, parts (a) through (j), present the results obtained. Note that to better relate to the constant structure Mohr envelope, *Fig. 11* shows I_m versus the average effective stress, $\bar{\sigma}_t'$, of the pieces of the CSME defined by the two Mohr circles obtained at each strain in an IDS-test (see *Fig. 4*). *Table 6* presents the legend for the various symbols used in *Fig. 11*.

Fig. 11 presents overwhelming evidence that all the soils tested possess a fundamental shear resistance behavior that, when probed by the IDS-test over the stress ranges investigated, produces I_m that varies linearly with CSME effective stress. *Fig. 12* presents a summary of the various linear relationships detailed in *Fig. 11*. Note the remarkable similarity in the slopes of most of the linear relationships summarized in *Fig. 12*.

Table 6. Legend for various symbols in Fig. 11.

Large symbols, such as ⊙, denote compression IDS-tests using strain-controlled triaxial equipment and single specimen, 2-curve, rigid load cell technique.

Small symbols, ⊙, denote less reliable tests using an earlier technique.

△ denotes special two-specimen IDS-tests (Schmertmann, 1962a).

Open symbols, such as ⊙, denote saturated specimens, except that ⊡ denotes dry specimens.

Crossed symbols, such as ⊠, denote partially saturated specimens.

Shaded symbols, such as ⊗³, denote deliberately overconsolidated specimens, with adjacent number denoting the hydrostatic overconsolidation ratio prior to the IDS-test.

⊙ denotes that a special consolidation procedure, other than 1-increment, hydrostatic, was employed prior to the IDS-test.

✕ denotes direct shear tests performed on dry sand at the Norwegian Geotechnical Institute in 1963.

5.2 CONSIDERING I AT ANY STRAIN

Section 5.1 treated only the maximum value of the I component, I_m. Almost all IDS-tests have shown that I_m usually occurs at very low strain. Each of the individual tests reported in each of the various parts of *Fig. 11* probably had its I_m occur at about the same low strain for all tests in that part. However, I_m was taken at whatever strain it occurred and *Fig. 11* includes no specific attempt to treat strain as an independent variable.

K.-H. Ho (1971) showed that a linear relationship between I and $\bar{\sigma}_t'$ existed at all strains investigated in each of the three artificial soils he tested. *Table 7* summarizes the results from his tests on duplicate specimens of remolded normally and overconsolidated kaolinite,

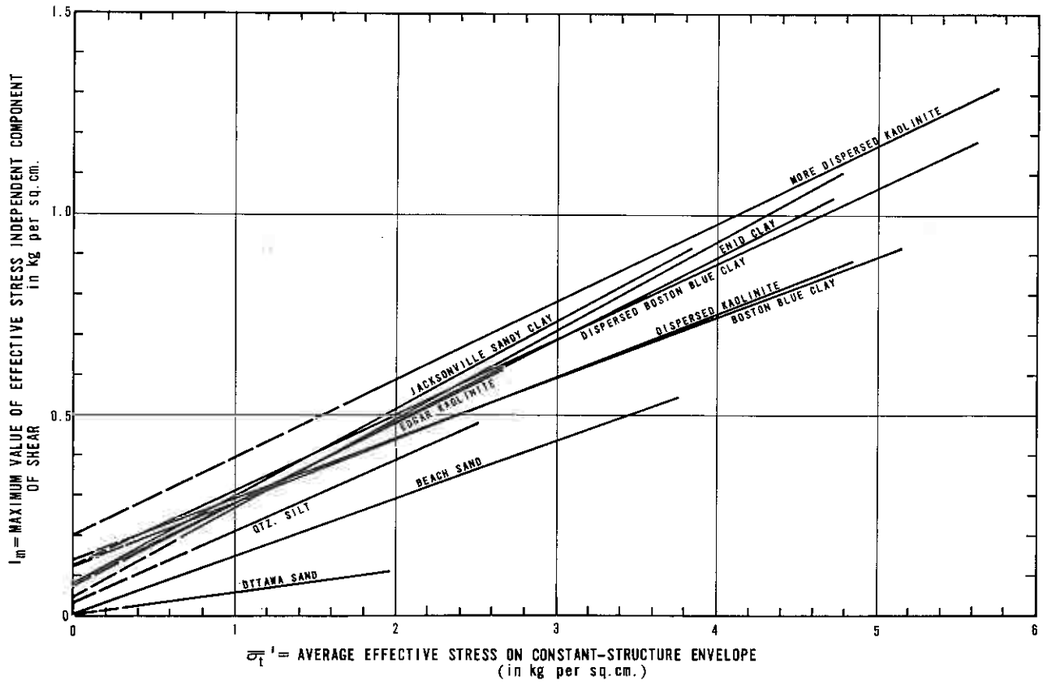

Fig. 12. Summary of linear I_m behavior for all soils investigated.

Table 7. K.-H. Ho's test to check linearity of I_ε vs. σ_t' at any strain.

Soil	Type IDS-test	No. tests in series	Av. linear correl. coeff.*	ε_1 values checked (%)
NC kaolinite	const – σ_1'	13	0.97	1, 2, 3, 4, 5
	– $(\sigma_1' + \sigma_3')/2$	6	0.96	1, 2, 3, 4, 5
	– vol.	3	0.98	1, 2, 3, 4, 5
OC kaolinite	const – σ_1'	3	0.98	1, 2, 3
	– $(\sigma_1' + \sigma_3')/2$	3	0.99	1, 2, 3, 4, 5
	– vol.	3	0.99	1, 2, 3, 4, 5
Cemented glass beads	const – σ_3'	9	0.94	0.5, 1, 1.5, 2

* Range for all tests at all strains = 0.92–1.00.

and also on duplicate specimens of glass beads cemented with "hydrocal". He used small-sample statistical theory and computed the correlation coefficients for the least-squares linear relationship between I and $\bar{\sigma}_t'$. He found for both soils, and with each of the four different types of IDS-tests he used, and at all strains investigated (including well past the strain of I_m) that the correlation coefficients varied between 0.92 and 1.00. *Table 7* lists the average values of correlation coefficient for the 3 to 5 levels of constant strain considered in each test series. He concluded that in all of his tests I_ε vs. $\bar{\sigma}_t'$ was linear at every strain investigated.

Although Ho did not prove the generality of this linear relationship at every strain for all soils, he did prove the principle that this linearity exists for at least some soils. The writer has little doubt it exists for most soils.

6. The shape of the CSME

6.1 THE SHAPE EQUATION

Equation (1) describes the piece of the CSME illustrated in *Fig. 4:*

$$\tau_\varepsilon = I_\varepsilon + d_\varepsilon \sigma_t' \quad \ldots\ldots\ldots\ldots\ldots (1)$$

Equation (2) expresses the slope of this piece of envelope:

$$d_\varepsilon = \frac{d\tau_\varepsilon}{d\sigma_t'} \quad \ldots\ldots\ldots\ldots\ldots (2)$$

The data on *Fig. 12,* which summarizes the various parts of *Fig. 11,* show clearly that the I-component behaves in accord with equation (3)

$$I_\varepsilon = (I_0)_\varepsilon + \beta\sigma_t' \quad \ldots\ldots\ldots\ldots\ldots (3)$$

Putting equations (2 and 3) into (1), and dropping the understood ε subscript, produces:

$$\tau = I_0 + \beta\sigma_t' + \sigma_t' \frac{d\tau}{d\sigma_t'} \quad \ldots\ldots\ldots\ldots\ldots (4)$$

from which:

$$\frac{d\tau}{d\sigma_t'} = \frac{\tau - \beta\sigma_t' - I_0}{\sigma_t'} \quad \ldots\ldots\ldots\ldots\ldots (5)$$

Solving Equation (5) produces the equation (6), which expresses the shape of a constant structure Mohr envelope over the stress range in which Equation (3) holds:

$$\tau = I_0 + \alpha\sigma_t' - \beta\sigma_t' ln\, \sigma_t' \quad \ldots\ldots\ldots\ldots\ldots (6)$$

Equation (6) seems like an unlikely expression for a shear resistance envelope. Its slope becomes infinite at the $\tau_t' = 0$ axis and becomes zero and negative at high values of σ_t'. *Fig. 13(a)* illustrates the CSME shape using I_0, α and β values more or less typical of those obtained from IDS-tests on remolded clays. *Fig. 13(b)* blows up the low-σ_t' range of this CSME.

Fig. 13(a) indicates the approximate maximum $\sigma_t' = 5.0$ kg/cm² used on clays for which this shape CSME applies. It appears that this CSME would not be reasonable for σ_t' over 7 kg/cm². This does not necessarily mean

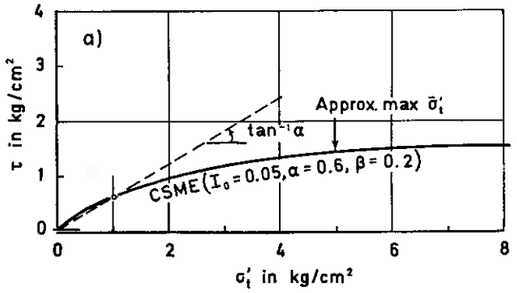

Fig. 13. Illustration of the high and low effective stress CSME shape typical of remolded clays.
a) Full stress range eqn. 6 applicable. b) The very low stress range.

an error exists in Eq. (6). It may mean that the particular structure described by this CSME cannot exist, or at least cannot mobilize additional shear resistance, at σ_t' greater than 7 kg/cm² – due, for example, to excessive crushing at the grain contacts. Also consider equation (7) in the next Section 6.2.1. The slope of this CSME remains reasonable to extremely high σ_m' – much beyond the stress levels which will produce extensive breaking of the grains.

Fig. 13(b) shows that the CSME appears reasonable at least to the minimum σ_t' level that effective stress compression, constant-σ_1' IDS-tests can probe – as shown by the smallest possible Mohr's circles and the piece of the CSME so determined. Note that several clays were tested down to near-minimum possible $\bar{\sigma}_t'$ levels (Fig. 11(a), (b), (f)) and equation (3) appeared to remain valid. The very steep slopes near the $\sigma_t' = 0$ axis predicted by Eq. (6) only occur very near the axis and have no significant effect on any test interpretations made herein.

The dimensionless α and β terms in equation (6) quantify very different aspects of soil structure. As described further in Section 10.2, β seems to be a grain-contact crushing constant. Its value does not change with the pressure units used for I_0 and σ_t'. But, α seems to depend on the soil friction, dilatency and dispersion aspects of structure. As shown in *Fig. 13(b)* one can also think of α as a reference $(\Delta\tau/\Delta\sigma_t')$ expressed by the secant d_ε over the $\sigma_t' = 0$ to 1 interval. Its magnitude depends on the units used for σ_t'.

6.2 INDEPENDENT EXPERIMENTAL CHECKS OF CSME SHAPE

6.2.1 *de Beer tests*

As noted in Section 2., E. E. de Beer (1965) has already presented data which at least approximately defined CSMEs, but which he called "intrinsic curves". This writer reconstructed intrinsic curves from de Beer's Fig. 1 and 6 for the two reassembled sands he investigated. These intrinsic curve envelopes apply only to the failure condition from drained, triaxial compression tests. Furthermore, de Beer defined his effective stress coordinate as the mean, or octrahedral, effective stress, σ_m'. After carefully plotting the intrinsic curves from his data, the writer constructed tangents graphically to these curves and obtained the I-component intercepts with the $\sigma_m' = 0$ axis. Because the envelope represents a drained failure condition, denote the I-component as I_{df}. For all cases checked I_{df} started at 0 when $\sigma_m' = 0$ and then increased approximated linearly with σ_m' at a slope whose tangent (= β in equation (6)) varied between 0.04 and 0.06. Equation (6) fits the de Beer intrinsic curves rather well. For example, Equation (6) in the form:

$$\tau = 0.87\, \sigma_m' - 0.05\, \sigma_m' ln \sigma_m' \quad \ldots\ldots\ldots\ldots\ldots (7)$$

fits the data for Molsand at $n = 38.9$ % as measured by the comparative secant angels presented in *Table 8.* The comparative agreement demonstrates how very well equations (6) and (7) match the shape of this real, but perhaps only approximate, CSME. The writer obtained equally good agreement using $\alpha = 0.97$ and $\beta = 0.06$ at $n = 36.5$ %, and $\alpha = 0.69$ and $\beta = 0.035$ at $n = 44.0$ % in this sand. Note that σ_m' probably does not differ greatly from σ_t' in conventional triaxial testing with $\sigma_2' = \sigma_3'$.

Table 8. Comparison of de Beer's intrinsic curve shape and that predicted from Equation (7).

σ_m' (kg/cm²)	Curve secant φ' (degrees)	
	de Beer	Eqn. (7)
0.1	45.0	46.1
2.0	40.3	40.7
50	34.0	33.8

J. Brinch Hansen (1967) also found de Beer's data interesting and developed an empirical equation especially to fit his intrinsic curves. However, equation (6) using the α and β values listed above, fits the de Beer data equally well.

6.2.2 *IDS-tests using different $\Delta\sigma_1'$ curve-hopping levels*

The CSME has a continually changing slope, as indicated by equation (5). Then, as illustrated in *Fig. 14* using an expanded τ scale for clarity, the larger the curve hopping $\Delta\sigma_t'$, the smaller the I-component. The relative magnitude of the I-component obtained using different levels of $\Delta\sigma_t'$, compared to some reference level, can be predicted by appropriate use of equation (6). Such a mathematical prediction can then be checked experimentally to verify or refute the reasonableness of equation (6). *Table 9* presents a comparison of mathematical and experimental I-component ratios referenced to a standard $\Delta\sigma_1'$ of 20 % (often used in constant-σ_1' IDS-tests). The very good agreement between such use of equation (6) and experiments further supports the validity of the CSME shape equation (6).

The use of Equation (6) also permits computing the error in the I-component that occurs when extrapolating to the $\sigma_t' = 0$ axis on the basis of a secant approximation of the curved piece of the CSME determined in an IDS-

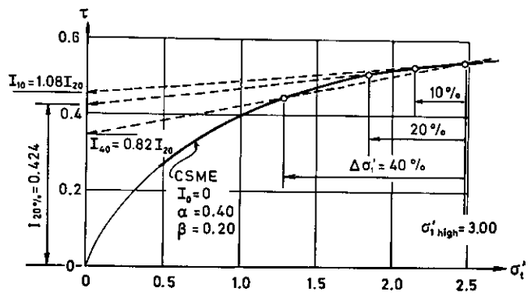

Fig. 14. Example of how the magnitude of the effective stress curve-hop in an IDS-test affects the I-component according to equation (6).

test (secant through points 1 and 2 in *Fig. 14*), vs. extrapolating using the correct tangent to the curve at the $\overline{\sigma}_t'$ stress mid-between points 1 and 2. Such a computation when $\Delta\sigma_1' = 20$ % shows the use of the secant approximation produces an *I*-component about 1.5 % too low, considered negligible in this study.

6.2.3 *Direct, single-specimen determination of the CSME*

As demonstrated by Strømann (1971) it appears possible in at least some soils to generate, from a single specimen, a complete constant structure Mohr envelope. This test, called the CSE-test by Strømann, consists of the following steps:

1. Perform a conventional drained triaxial test to some desired strain condition. Use a very rigid load cell.
2. Permit the test specimen to reach some specified almost-equilibrium state with the load by allowing additional strain, as required, at constant load.
3. Increase pore water pressure to some maintained-constant value, while also keeping cell pressure constant.
4. The resulting reduction in σ_3' will cause a reduction in the deviator stress the specimen can sustain. The force exerted by the load cell will eventually decrease until reaching a new equilibrium. This new equilibrium defines the maximum shear resistance that the given structure can mobilize at its new effective stress condition.
5. Repeat steps 3 and 4, each time producing a new equilibrium condition at a reduced σ_3', and therefore also a reduced shear resistance capability for that soil structure. Repeat these steps until placing an effective stress Mohr circle as close to $\sigma_3' = 0$ as practical.

Each of the above steps produces an almost-equilibrium condition which one can then represent by an effective stress Mohr circle. Strømann used the initial equilibrium condition, plus four steps in the direction of reduced effective stress, to define five Mohr circles. She then graphically fitted a tentative CSME over these circles to obtain points of tangency with each. These points then formed the basis for a least-squares fit of equation (6) through the five points thus obtained.

Table 9. Comparison of measured effect of magnitude of effective stress curve-hop in constant-σ_1' IDS-tests with effect predicted from Eqn. (6).

$\frac{\Delta\sigma_1'}{\sigma_1'_{high}}$ %	$I_m/(I_m$ when $\Delta\sigma_1' = 20$ %)			
	Eqn. (6)	Remolded		Undisturbed sandy kaolinite
		Kaolinite ($I_0 = 0.08$)	Enid clay ($I_0 = 0.07$)	
10	1.09	1.15	1.12	
20	1.00	1.00	1.00	1.00
30	0.92	0.91	0.86	
40	0.81			0.75
60	0.60			0.58

The curves from the graphical fit and those obtained from equation (6) matched so well that a graphical comparison would make any separation difficult to see. Instead, consider the comparative information presented in *Table 10:* First note the very high curve-fit correlation coefficients, which confirms the excellent fit provided by Equation (6) for the envelopes obtained directly from the CSE-tests. Because Ho (1971) tested these same soils, *Table 10* also includes a comparison between I_0, α and β obtained by Ho using the IDS-test method (Section 7.3) compared with I_0, α and β obtained from the best-fit Equation (6) to the CSE-tests. The agreement seems reasonable and further confirms the validity of the CSME equation (6).

The CSE-test as described above allows a small amount of additional axial strain to take place as the load against the load cell diminishes with decreasing effective stress and the load cell, fixed only at one end, compresses the sample specimen slightly with this release. *Table 10* includes the axial compressive strain at the initial equilibrium (after step 1) and the final strain at the 5th, σ_3' almost 0, equilibrium condition. The difference between these strains varied from 0.09 to 0.16 %. The CSE-test as presented assumes this additional strain, as well as any unmeasured changes in radial strain, produces a negligible change in the soil structure during this method of probing that structure's ability to mobilize shear resistance at varying levels of effective stress. The CSE-test may not prove suitable for soils that swell appreciably during the large effective stress reduction in this type test, and thus perhaps significantly change structure during this reduction.

Strømann's experience with the CSE-test also indicates that the investigator must allow considerable time to reach her specified almost-equilibrium state after each step reduction of effective stress (change in deviator stress per hour less than 1 % of total change during each step reduction). She required a total of 4 days for the 5-step tests on glass beads and 7 days for kaolinite.

6.3 CONCLUSION REGARDING SHAPE

From the success of the independent checks described in 6.2.1 and 6.2.2, and 6.2.3 it seems well established that Equation (6) adequately describes the shape of the CSME for the range of soils and stress levels investigated. However, the experiments described herein provide only limited data on soils with *PI* exceeding 45 %. Such clays, especially if they present swelling complications, may, or may not, behave differently from equation (6).

7. Determining the bond shear resistance from the CSME

7.1 DEFINITIONS

As introduced in Section 2., the CSME illustrated in *Fig. 1* has an intercept with the $\sigma_t' = 0$ axis. This intercept, denoted I_0, must represent the shear mobilization capability, when $\sigma_t' = 0$, of the soil structure whose CSME produces that I_0 intercept. The writer assumes that any shear resistance at this condition must result from internal particle--particle bonds within the soil. This research does not distinguish between the many possible causes of such internal bonds, but simply sums their effects and designates the total mobilized bond resistance as I_0. For a given soil, following a given stress path, I_0 attains some maximum value, $I_{0(max)}$, denoted I_b for simplicity. I_0 represents the mobilized bond shear resistance and I_b the bond shear strength. As with any other shear resistance component, I_0 and I_b may be path dependent.

The writer recognizes that a more fundamental explanation for friction behavior relates friction to the stress-dependent making and breaking of the numerous atomic bonds that form between materials forced into contact. Mitchell (1976) shows that such fundamental thinking can help explain soil strength behavior in engineering problems. However, in this paper the writer chose the term "bonds" as used in the engineering sense to refer to the origin of that part of a soil's shear strength still available when the engineering effective stress = 0.

Table 10. Comparison of CSME-data obtained from CSE-tests and from IDS-tests.

Soil	From Strømann's CSE-tests							From Ho's IDS-tests			
	ε_1 %		Least sq. fit of eqn. (7)					Type			
	Start	End	No. points	I_0 (kg/cm²)	α	β	Correl. coeff.		I_0 (kg/cm²)	α	β
									($\varepsilon_1 = 1$ to 4 %)		
NC glass beads	0.46	0.61	5	−.013	0.60	0.07	.9992	const − σ_3' NC	−.08 to +.02	0.60	−.01 to +.06
$\sigma_3'_{initial} = 1.0$ kg/cm²	0.95	1.05	5	−.015	0.63	0.04	.9999				
Kaolinite OCR = 2	0.83	0.92	5	.010	0.26	0.08	.9997	const − $\left(\frac{\sigma_1'+\sigma_3'}{2}\right)$OC	0.01 to 0.03	0.20 to 0.37	0.17
$\sigma_3'_{initial} = 1.0$ kg/cm²	2.13	2.29	5	.011	0.32	0.13	1.0000				

7.2 THE CSE-TEST METHOD

As described in Section 6.2.3, some soils permit a direct determination of the CSME to almost the $\sigma_t' = 0$ intercept. One can then find the intercept by fitting Equation (6) through the part of the CSME obtained from the CSE-test and using the resulting formula to obtain the value of I_0. *Table 10* includes I_0 values obtained by this method and they agree approximately with those obtained by Ho (1971) using the IDS-test methods described in the next section.

7.3 THE IDS-TEST METHOD

The IDS-test produces only a small piece of the CSME, but does this for a spectrum of CSMEs as these develop with continuing strain. In Section 5 the writer presented experimental results that seem to prove that the *I*-component varies linearly with effective stress over the full range of effective stress investigated, including as close to the $\sigma_t' = 0$ axis as feasible in our experiments. Furthermore, as strongly suggested by the evidence in Section 4, the *I*-component at a given σ_t' appears independent of all structure-change variables investigated. The CSME of course changes with changing structure, but not the *I*-component at a constant σ_t' in strain controlled testing.

We wish to obtain the CSME intercept I_0. Because *I* varies linearly with σ_t' and independently of soil structure, it follows that one can obtain *I* from the same soil at a variety of structures at any σ_t'. A linear extrapolation to $\sigma_t' = 0$ then produces I_0.

Thus, all the intercepts with the $\overline{\sigma}_t' = 0$ axes in *Figs 11* and *12* represent bond shear resistance values – in these cases bond strength, at least approximately, because of the use of I_m. *Table 11* lists the various values of approximate bond strength obtained from these tests on remolded soils. Considering inevitable experimental error, these results seem very reasonable, at least for the non-plastic soils. The I_b values in the remolded clays vary from 0.05 to 0.20 kg/cm². I_b does not seem to relate to clay *PI*. The kaolinite tests show a definite trend of increasing I_0 with dispersion (see *Table 1*), but dispersing Boston blue clay had an inconclusive effect.

Note that the IDS-test method of obtaining I_0 and I_b involves a 2-level elimination of the effects of effective stress – the first to obtain each *I*-component and the second when extrapolating for I_0 from the I-σ_t' linear relationship. Each IDS-test obtains information about *I* over the full range of strain in such a test. An investigator ordinarily would need at least 2 IDS-tests to perform the

Table 11. I_{0m} bond strength in some remolded soils.

Soil *	PI (%)	Bond strength (kg/cm²)
DWEPK	21	0.08
N-EPK	7	0.13
Q-EPK	4	0.20
BBC	19	0.14
Q-BBC	11	0.13
Enid	9	0.07
JSC	14	0.05
Qtz. silt	NP	0.03
Beach sand	NP	0.01
Ottawa sand	NP	0.00

* These soils are described in more detail in Tables 4a and 4b.

extrapolation for I_0. On the other hand, the CSE-test requires only a 1-level elimination of the effects of effective stress to extrapolate for I_0, but at only one strain. However, the CSE-test can be repeated on the same specimen brought to a new, greater strain after each test.

7.4 USING THE IDS-TEST METHOD ON UNDISTURBED SOILS

This section presents a number of examples of the use of the IDS-method to determine I_0. The first example reports on tests with artificially prepared quartz silt. The remainder involve undisturbed samples using, in part, data from other investigators who perhaps inadvertently performed IDS-tests. Only the test series on the Manglerud clay had the specific intent of determining bond strength.

7.4.1 *Partially saturated quartz silt*

The I_m-σ_t' results reported in *Fig. 11, part (h)*, came from either dry or completely saturated specimens of a reassembled quartz silt. We also tested this silt in a partially saturated state. One group of 5 constant-σ_3' IDS-tests on this silt had dry densities and degrees of saturation within the relatively narrow range of 74.1 to 79.4 pcf and 17.4 to 19.6 % respectively. *Fig. 15* shows the I_m vs. $\bar{\sigma}_t'$ results from these tests, together with the β-slope determined from *Fig. 11(h)*.

Of course, the capillary attraction forces resulting from partial saturation produced an apparent bond in the partially saturated specimens. Assuming the β-slope through the partially saturated tests equals that through the dry and saturated tests, and extrapolating to the $\bar{\sigma}_t' = 0$ axis, produces an I_{m0} intercept $\approx I_b = 0.27$ kg/cm². As also shown in *Fig. 15*, this results from a capillary effective stress of 1.5 kg/cm². This example shows how an engineer might by this method evaluate the apparent bond contribution of partial saturation or the equivalent effective stress due to partial saturation.

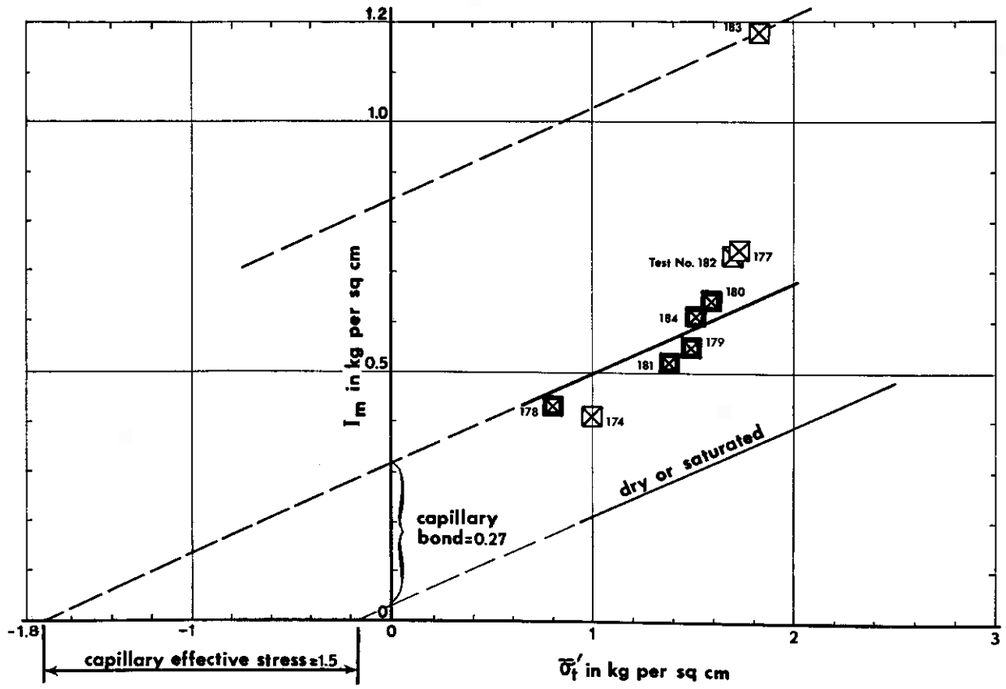

Fig. 15. I_b determination in compacted, partially saturated, ground quartz silt, 100 % passing 325 sieve.

7.4.2 *A natural cemented sand*

The writer cut specimens for constant-σ_3' IDS-tests from an undisturbed block of air-dry, medium to coarse sand, cemented with 5 % kaolinite, which he obtained from the vicinity of Tupelo, Mississippi, U.S.A. For a further description of this soil, as well as example IDS-test data, see Schmertmann (1962b, pp. 173, 179). Although no two specimens from this natural block of soil could be considered identical due to obvious variability in cementing, 6 of the specimens appeared similar with initial void ratios varying between only 0.72 and 0.82 and degrees of saturation between 2.7 and 9.8 %. *Fig. 16* presents the

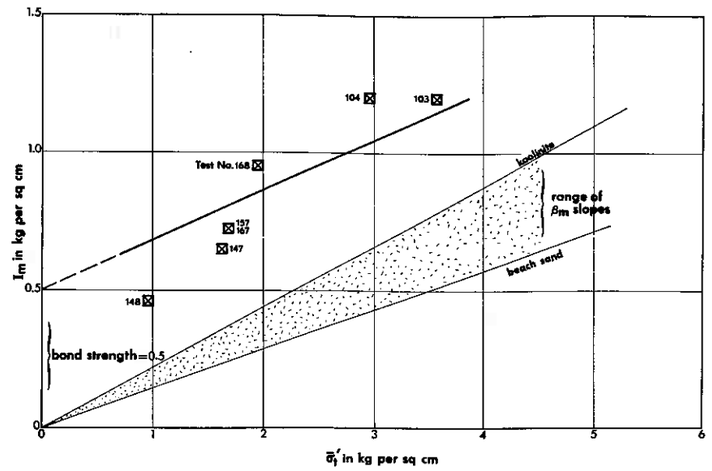

Fig. 16. I_m determination from undisturbed Mississippi cemented sand, 3–13 % partial saturation.

I_m vs. $\bar{\sigma}_t'$ results from these tests. As shown, using a β-slope equal to that previously obtained from beach sand (*Fig. 11, part (i)*) produces an $I_{m0} \approx I_b = 0.50$ kg/cm². Another, seemingly similar, specimen had an unconfined compressive strength of 3.2 kg/cm². This example demonstrates the method can also evaluate bond strength in a brittle, cemented soil.

This series of tests presented a demonstration that even very weak and very sensitive clays could have their bond shear resistance investigated by IDS-tests of a suitable type and performed with suitable care. Note that the β-slope in *Fig. 17*, equal to about 0.17, fits well within the range of 0.15 to 0.22 observed in *Fig. 12* for remolded cohesive soils.

7.4.3 *Undisturbed Norwegian quick clay*

As noted in the introduction to section 7.4, this series of tests had the specific purpose of evaluating bond strength. The soil tested was Manglerud quick clay, which the NGI used previously, and subsequently, as a test clay for research purposes. This series consisted of 6 constant-volume IDS-tests, 5 in conventional triaxial compression and 1 in simple, direct shear. NGI personnel obtained these samples and handled them with great care. The pore pressure measurement system employed a back pressure of 6.0 kg/cm². The strain rate was held at ½ % per day axial compression, and the difference between the two constant-volume states of the soil was about $^1/_{200}$th specimen total volume. The interested reader can find all the details from these tests in an NGI Internal Report by Schmertmann (1963d).

Fig. 17 presents the results in I vs. $\bar{\sigma}_t'$ plot using expanded scales. Each different shaped symbol represents a different test. The smaller, lighter form of the symbol denotes data obtained at strains less than undrained shear failure. A dashed line connects these points until reaching the largest, emphasized point, which denotes the I-component at undrained failure. Based on these results, the writer concluded that bond shear resistance at undrained failure, I_{0u}, in this quick clay equalled essentially 0.00 kg/cm², and probably equalled no more than 0.01 kg/cm² prior to this failure. Note that the undrained shear strengths in these tests were low, varying from 0.12 to 0.33 kg/cm², with failure strain between 1.1 and 2.6 %.

7.4.4. *Two normally consolidated clays tested by "perfect sampling" IDS-tests*

The perfect sampling procedure as described, for example, by Noorany and Seed (1965) involves the testing of two specimens of clay before and after a simulated, perfect sampling procedure in the triaxial chamber. The procedure produces two specimens at almost the same structure but with different initial effective stress conditions. Comparing stress-strain behavior between the two specimens during subsequent undrained compression tests thus represents, in effect, a two-specimen version of a constant-volume IDS-test. Schmertmann (1965b) discusses this equivalency in more detail.

Noorany and Seed (1965) investigated undisturbed samples of the San Francisco Bay mud in this manner and presented their results in sufficient detail for the writer to extract those data needed for an I_0 extrapolation at undrained failure in this clay. Using these authors' data (their Figures 22, 23 and Table 4) the writer obtained the points plotted in *Fig. 18* herein. Note that these points fall very close to a straight line, as expected. This line has a β-slope = 0.20, also within the expected range. Extrapolating these data points to the $\bar{\sigma}_t' = 0$ intercept produces a bond resistance at undrained failure, $I_{0u} =$ 0.07 kg/cm².

Ladd and Lambe (1963) presented the data from a similar set of perfect-sampling tests using normally consolidated clay from Kawasaki, Japan. These authors also provided sufficient information to use their test data to

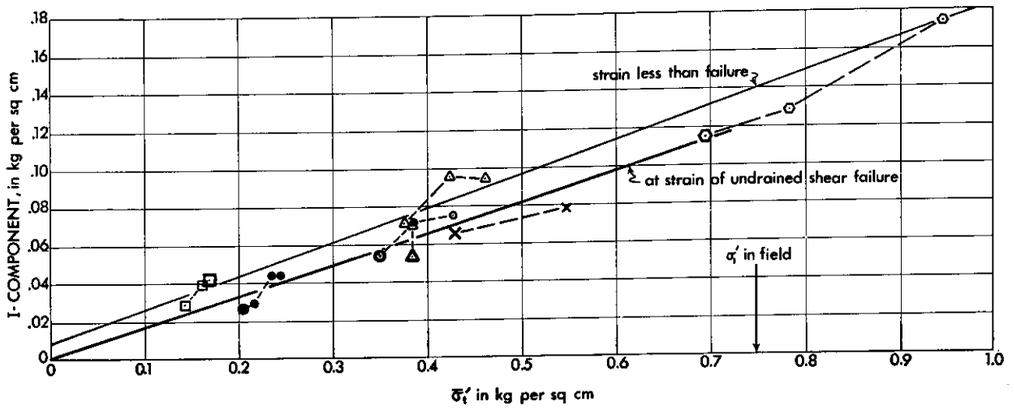

Fig. 17. I_{ou} determination from I component results from undisturbed Oslo quick clay.

arrive at an estimate of bond shear resistance at undrained failure – presented herein as *Table 12*. Plotting the results in *Fig. 19* again produced the expected linear relationship, with an extrapolation to the very similar I_{0u} value of 0.06 kg/cm². The β-slope equals a somewhat high 0.24, but part of the reason for this is that the $\Delta\sigma_1'/\sigma_1'_{high}$ ratio was only about 11 % instead of the 20 % used for most tests in *Fig. 12*. As shown in Section 6.2.2 this will increase I-values, and therefore β, about 10 %. A 10 % reduction from 0.24 = 0.22, which reaches the upper limit of 0.15 to 0.22 from the reference tests on remolded cohesive soils.

The reader can obtain much more detailed data concerning the properties of these clays from the original references cited. However, it's of interest here to note that their *PI*'s ranged from 30 to 45 %, and thus seem to extend the validity of the IDS-test concepts to higher *PI* clays than otherwise reported herein.

As shown in subsequent Section 8, the bond shear resistance values of 0.06 and 0.07 kg/cm² appear quite reasonable in light of other evidence.

7.5 AN APPROXIMATE, ONE SPECIMEN METHOD

The IDS-test method for extrapolating for I_0 described in 7.3 and 7.4 requires a series of at least 2 comparative tests on the same soil. Errors can result from the inevitable differences between supposedly duplicate specimens. Random errors are less serious provided one tests enough specimens. However, systematic errors might also occur, such as a progressive destruction of cementation bonds when consolidating to higher effective stresses prior to IDS-testing, or progressive swell-destruction of bonds resulting from progressive reduction of effective stresses prior to IDS-testing. For such reasons, as well as economy, consider the following 1-test method for estimating I_0.

Study of *Fig. 12* shows that the β-slope values for remolded soils appear to vary over a rather limited range. For instance, β varies from 0.15 to 0.22 for cohesive soils. The undisturbed clay tests reported in 7.4.3 and 7.4.4 also fit this range. *Fig. 20* illustrates this slope variation, with the average value of 0.185 indicated. Also plotted on this figure are the 1-test I_m values from

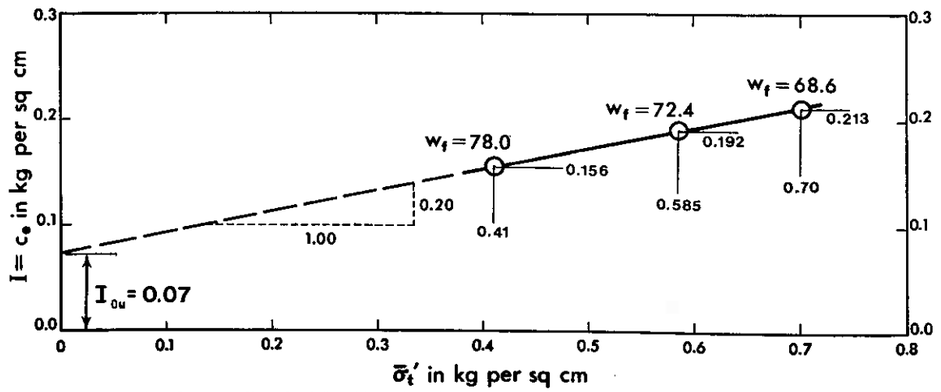

Fig. 18. I_{ou} determination from undisturbed San Francisco Bay mud at undrained failure (approx. constant-volume IDS-tests, Noorany and Seed 1965).

Table 12. Data from Ladd and Lambe (1963) on Kawasaki Clay for Fig. 19 (all stresses in kg/cm²).

Clay layer	Type test	From author's Fig. 2, at failure $\frac{\sigma_1-\sigma_3}{2}$	$\frac{\sigma_1'+\sigma_3'}{2}$	Computed σ_t'	$\bar{\sigma}_t'$	I
I	CA-$\overline{UU}$	1.07	1.84	1.47	1.64	0.458
	$\overline{CAU}$	1.21	2.24	1.82		
II	CA-$\overline{UU}$	1.92	3.44	2.77	2.92	0.764
	$\overline{CAU}$	2.03	3.79	3.08		
III	CA-$\overline{UU}$	2.88	5.16	4.16	4.48	1.156
	$\overline{CAU}$	3.14	5.90	4.81		

two constant-σ_1' IDS-tests on undisturbed clays. In the absence of better information on the β-slope applicable for each clay (such as in Fig. 11(d) for the BBC), an investigator can assume the average value. Then the vertical distance between the 1-point test and this average slope, or a more applicable slope if available, represents the estimated I_b value for each of these clays.

8. Comparing I_0 with other methods

Now consider the very important test of how the bond resistance values discussed in Section 7 compare with results using other methods of predicting or estimating the fundamental cohesive strength component. The writer will now consider three such methods in order of increasing sophistication, ending with Rowe's beautiful stress-dilatency method.

8.1 JAKOBSON'S ORIGIN COHESION

Jakobson (1953)proposed a field vane method that may produce a result closely related to the I_{0u} bond shear resistance. He first performed a series of vane tests with depth at several sites in Sweden where he found uniform,

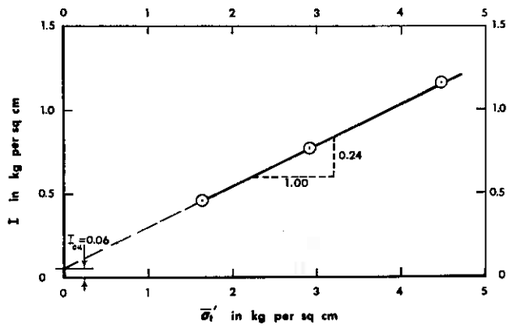

Fig. 19. I_{ou} determination from undisturbed Kawasaki clay at undrained failure (approx. constant-volume IDS-tests. Ladd and Lambe 1963).

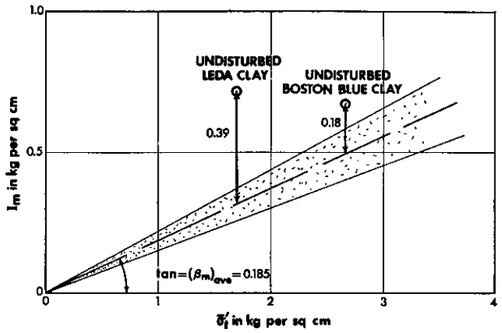

Fig. 20. Possible bond strength test using only one specimen.

soft, normally consolidated clays with an underwater surface. He found the now well known linear variation of undrained shear strength with depth. A short extrapolation to the surface then gave him the undrained vane shear strength at a point of zero, pre-vane, effective stress. He termed this strength the "origin cohesion". In all three examples he reported origin cohesion between 0.05 and 0.08 kg/cm². Subsequent similar data by others show such values as typical for post-Pleistocene clays. Note that Jakobson reported magnitudes of origin cohesion similar to those noted in *Table 11*. More important, note that the I_{0u} values of 0.07 and 0.06 kg/cm² reported in 7.4.4 for the undisturbed San Francisco and Kawasaki clays fall exactly within the range of Jakobson's origin cohesion.

In this method let us assume that everything (meaning initial effective stress, the effective stress changes due to vane insertion and rotation, the difference in soil structure as a result of varying effective stress, etc.) varies linearly with depth. Then extrapolating to the surface should produce the undrained strength at zero effective stress, and therefore the bond shear resistance at undrained vane failure.

The writer had the opportunity to try Jakobson's origin cohesion method in San Francisco Bay mud, but in clay somewhat different than that tested by Noorany and Seed (1965). *Fig. 21* presents the results from 5 vane shear depth profiles below a thin drying crust at a tidal flat site in San Francisco Bay. These very consistent results, obtained with the high-quality Jonell and Nilsson vane shear equipment, produce an origin cohesion of 0.09 to 0.11 kg/cm². Considering the possible difference in the clays (average water content 76 vs. 90 %, liquid limit 81 vs. 88 %, plastic limit 30 vs. 53 %, and average field vane sensitivity 5 vs. 9, when comparing the *Fig. 21* site with the N & S site), and the rate effects between field vane tests and N & S's laboratory tests, the writer believes 0.09 to 0.11 represents excellent agreement compared to 0.07 kg/cm² determined from *Fig. 18*.

8.2 TENSION TESTS

The writer (1972) performed a series of 16 hydraulic fracturing tests at three sites in Leda clay in Ottawa,

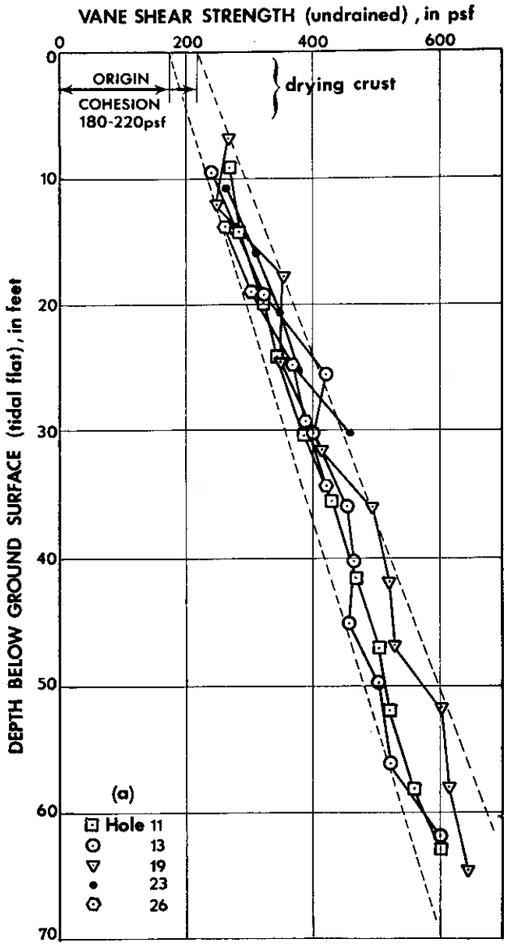

Fig. 21. Results from vane shear tests in San Francisco Bay mud illustrating determination of Jakobson's origin cohesion.

Canada. He assumed the difference between the hydraulic pressure required to begin radial cracks, and the total subsequent soil pressure required to close those cracks, as the tensile strength of this cemented clay. In these 16 tests this difference varied between 0.06 and 0.36, with an average of 0.19 kg/cm². Although the Leda clay with the *Fig. 20* I_b of 0.39 comes from a different site in the vicinity of Ottawa, a tensile strength of 0.19 seems reasonably compatible with $I_b = 0.39$ kg/cm².

Topshøj (1970) performed a series of axial extension, constant-σ_1', IDS-tests on remolded kaolinite and compared the extrapolated I_{m0} values with the shear resistance measured at $\sigma' = 0$ from effective stress tension tests as described by Bishop and Garga (1969). *Table 13* presents the results after a small-sample statistical analysis of her experiments.

Table 13 demonstrates clearly that the two independent experimental techniques arrived at about the same value of I_{m0}. Note also that I_{m0} determined by axial extension IDS-tests gave essentially the same bond shear resistance as axial compression IDS-tests of the constant-σ_1' type (0.08 kg/cm² in *Table 11*). The agreement improved further after correcting the Bishop tests, approximately, for the effects of progressive volume change during testing in accord with Rowe's stress-dilatency theory.

8.3 ROWE'S STRESS-DILATENCY METHOD

P. Rowe (1962) has proposed, and he and his colleagues have expanded upon, a comprehensive theory to correct laboratory shear strength test results for the internal and external energy demands associated with the volume change (dilatency) effects of soil structure. His work represents one of the few examples in soil mechanics of a major theoretical discovery later confirmed by experiments. In contrast, the writer's work presents experimental discoveries with attempts to fit a theory around them. Rowe's dilatency method compares a soil at different effective stress conditions after eliminating the effects of different soil structure by means of a mathematical technique. The writer's IDS-method attempts to eliminate soil structure effects by experimental techniques. Both approaches have their relative advantages and disadvantages. Both aim at evaluating the more fundamental shear strength behavior of particulate systems such as soil.

It is of course of great interest to compare results using these two very different approaches toward the same objective. K.-H. Ho (1971) compared the methods using duplicate specimens of three artificial soils. He very carefully performed IDS-tests of various types and at the same time made the very accurate volume change measurements required to make the Rowe stress-dilatency soil structure corrections. *Table 14* presents the comparisons that Ho obtained between I_0 and the Rowe interparticle cohesion parameter c_f (Rowe et al. 1964). *Table 14* further describes the same tests already reported in *Table 7*, but the I_0 and c_f values represent average values from all the strains considered in each case. *Table 14* demonstrates clearly that both methods produce about the same results in measuring the more fundamental cohesion parameters c_f and I_0, at least on the average.

Table 13. Topshøj's I_0 comparison between extension IDS-tests and effective stress tension tests using remolded kaolinite clay.

Type test	No. tests	I_{m0} (kg/cm²)	95 % confidence interval
Const-σ_1' axial extension	16	0.084	±0.025
G-B tension	11	0.112	±0.041
G-B tension with approx. stress-dilat. correction	11	0.084	±0.032

Table 14. Ho's comparison between average values of I_0 and stress-dilatancy c_f for all strains investigated.

Soil	Type test	Av. I_0 (kg/cm²)	Av. c_f (kg/cm²)	Av. $\varrho = 1 + \frac{\Delta\varepsilon_v}{\Delta\varepsilon_1}$
NC kaolinite	const – σ_1'	0.047	0.059	1.30
	const – $\frac{\sigma_1'+\sigma_3'}{2}$	0.103	0.051	
	const – vol.	0.088	0.128	
	all	0.080	0.079	
OC kaolinite	const – σ_1'	0.056	0.048	1.20
	const – $\frac{\sigma_1'+\sigma_3'}{2}$	–.018	0.033	
	const – vol.	0.143	0.165	
	all	0.061	0.082	
Glass beads	const – σ_3'	–.033	–.018	1.75
Cemented glass beads	const – σ_3'	0.228	0.140	1.50

Thus, two completely independent approaches to the same problem have yielded very similar results.

The reader familiar with stress-dilatency might well wonder why the IDS-tests produce seemingly accurate results for I_0 without applying stress-dilatency corrections to the IDS-test data. The small, approximately negligible, difference in soil structure between the two comparative effective stress situations in the IDS-test accounts, in part, for this success. The soil at both effective stress conditions has approximately the same dilatency rate at all strains. For example, *Fig. 22* illustrates this using one of Ho's tests on glass beads cemented with hydrocal. Ho and the writer have found similar parallel behavior in dilatency rates in all comparative tests. Thus, the Rowe dilatency correction factor $(1 + \Delta\varepsilon_v/\Delta\varepsilon_1)$, appropriately denoted ϱ herein, has at least approximately the same value for both the higher and lower effective stress conditions at any strain in an IDS-test.

A mathematical study of the problem produced the following equation:

$$I_{\text{corrected}} = I\,(\varrho)^{-1/2} \quad \ldots\ldots\ldots\ldots\ldots\ldots \quad (8)$$

Neglecting to correct the I-component for dilatency produces an error in I of 10 % or less over the range $0.92 \leqq \varrho \leqq 1.23$ and 20 % or less over the range $0.70 \leqq \varrho \leqq 1.56$. A $\varrho > 1$ means an increase in volume with strain and an equation (8) correction ratio of less than 1.00.

However, when it comes to the linear extrapolation for the I_0 value as in the many examples in Sections 7.3 and 7.4, the situation becomes more favorable because the stress-dilatency correction also changes σ_t' in the same direction as the I-component. *Table 15* presents the approximate error in I_0 one may expect due to neglecting the stress dilatency correction as made by Rowe. The actual error depends on the magnitude of I_0, the β-slope and the stress-dependent component d_e. *Table 15* suggests a relatively minor error in I_0 with soil structures having dilatency rates within the ordinary range.

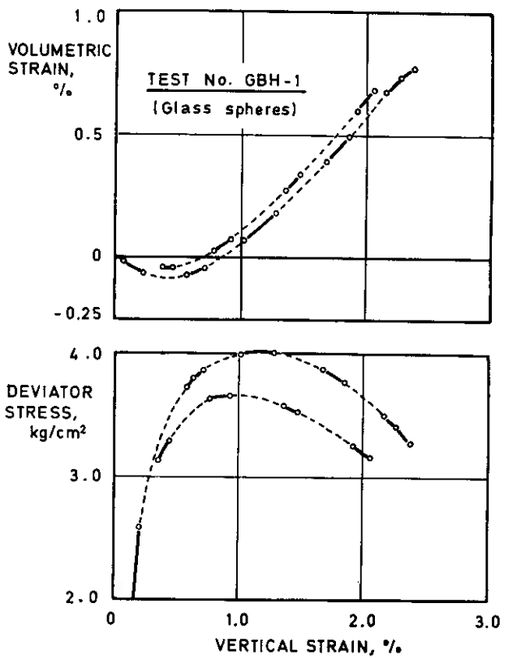

Fig. 22. Example illustrating the similar ϱ-dilatency correction at both effective stress levels in an IDS-test (from Ho 1971).

The last column in *Table 14* includes the approximate, average dilatency rate, $\varrho = 1 + d\varepsilon_v/d\varepsilon_1$, for some of Ho's tests. In all cases these average rates are positive and therefore, from *Table 15*, I_0 would be too-high as a result of neglecting the dilatency correction. But, *Table 14* indicates that in only three of the six cases does the average I_0 exceed $\bar{c}_f$. This comparison suggests that other factors have greater importance than the relatively minor effect of neglecting the stress-dilatency correction to I_0. Finally, K.-H. Ho (1971) did attempt dilatency corrections to I_0 but found no further improvement in the I_0–c_f comparison.

8.4 CONCLUSIONS ON COMPARISONS WITH OTHER METHODS

It seems clear from the general agreement success of these different alternate methods of estimating the bond shear resistance within cohesive soils that the IDS-test

Table 15. Approximate error in I_0 due to neglecting stress-dilatancy correction.

$\varrho = 1 + \frac{\Delta\varepsilon_v}{\Delta\varepsilon_1}$	Error in I_0
+2.0	15 % too high
+1.5	9 % too high
+1.0	No error
+0.75	7 % too low
+0.50	18 % too low

also provides an independent method for determining bond resistance. One can argue about the relative accuracy of one method vs. another, but they all deal with fundamental shear behavior. The IDS-test CSME method and the stress-dilatency method probably provide the most opportunity for learning about soil shear behavior and producing a practical spinoff.

9. Time-transfer of IDS-components

Dr. Bjerrum developed a special interest in how time effects relate to a soil's shear behavior. In Bjerrum (1973) he placed great emphasis on the observations by Schmertmann and Hall (1961a) concerning the time-transfer from the *I*-component to the *D*-component during anisotropic consolidation. P. Rowe (1957), also observed that the small, empirical effective stress cohesion intercept appeared to diminish with time. It is of course well known that clays increase undrained strength substantially with an increase in rate-of-strain. But, what do we know about rate-of-strain effects in the direction of low rates, especially with respect to the fundamental shear components?

9.1 RATE-OF-STRAIN EFFECTS

As discussed in 4.1.7, changing the time rate-of-strain in one set of comparative IDS-tests on remolded kaolinite produced only minor changes in the *I*-component but a dramatic increase in the strain-rate of mobilization of the D-component. The writer also observed similar comparisons during more causal observations of results from tests on other clays.

However, as shown by Schmertmann (1963a, p. 268 and Fig. 28), decreasing the average rate of strain in an IDS-test, by changing from a strain-controlled test completed in 1 day to a 10-increment stress-controlled test with 3 days per increment, produced a large transfer from *I* to *D*. This transfer increased with strain and time. Note that some of the strain-controlled tests discussed in 4.1.7 also took 30 days or longer. It appears that forcing the strain, even very slowly, tends to maintain the *I*-component, while allowing strain adjustment under constant stress conditions tends to transfer *I* to *D*.

9.2 PRIMARY AND SECONDARY CONSOLIDATION TIME EFFECTS

Section 4.1.4 has already presented a discussion of the non-importance of such time effects to the *I*-component. *Tables 4* and *5* indicated the time required for primary consolidation and the manner of performing this consolidation appeared to have no significant effect. *Fig. 10* shows that lengthening secondary time by a factor of about 600 had almost no effect on I_m. Once again, we observed a dramatic increase in the low-strain rate of mobilization of the *D*-component.

An important corollary result from progressively longer times in secondary compression is that such compression can produce a substantially stiffer soil structure. For example, Schmertmann (1965a) showed the initial tangent modulus from the testing of specimens similar to those reported in *Fig. 10* increased by a factor of about 10 as a result of longer secondary times. Bjerrum and Lo (1963) also observed such stiffening, but to a lesser degree, during aging of undisturbed samples of a Norwegian clay. The quasi-preconsolidation effect reported by Leonards and Ramiah (1960) provides further evidence of the low-strain structure-stiffening effect of increasing time in secondary compression. It appears that these important stiffening effects may have an association with the *I*- to *D*-component transfer occurring during secondary compression.

9.3 EFFECTS DURING ANISOTROPIC CONSOLIDATION

Schmertmann and Hall (1961a) reported on a comprehensive series of constant-σ_1' IDS-tests on remolded specimens of kaolinite and Boston blue clay after one-day anisotropic consolidation to various K' levels. L. Bjerrum (1973) took special note of these experiments. He had a special interest in the clearly demonstrated time transfer from the *I*-component to the *D*-component during the secondary compression phase of the K' consolidation. For example, consider *Figs 23(a)* and *23(b)* taken from the 1961 reference. In 1961 we still used the old test and component notation. These figures show, as explained in the reference, that after some secondary time following different levels of K' consolidation the deviator

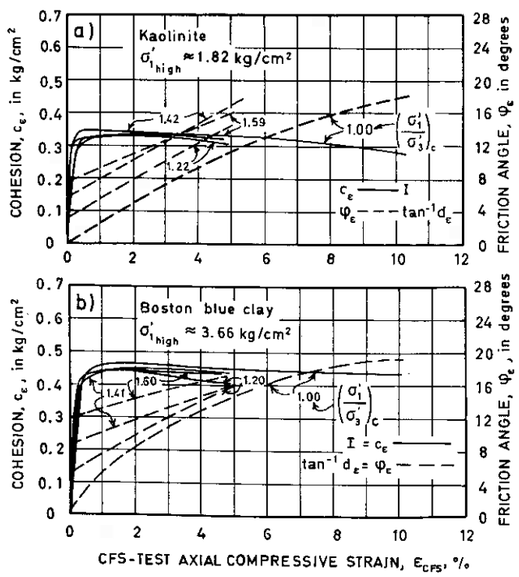

Fig. 23. The strain-mobilization of the *I* and *D* components after about 20 hours anisotropic secondary consolidation (from Schmertmann and Hall 1961a).

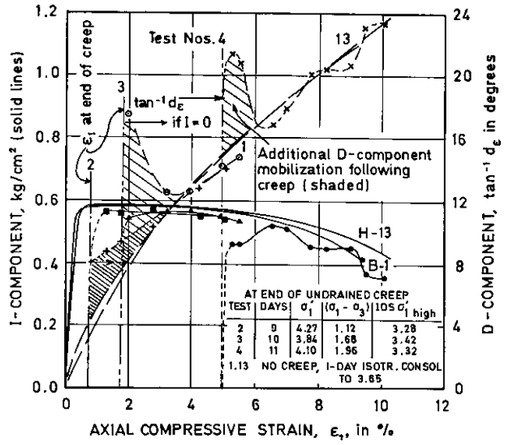

Fig. 24. Effect of undrained creep on shear component mobilization in remolded kaolinite (from Bea 1960).

stress transferred almost entirely to the *D*-component. Then, during the subsequent increase in strain and strain rate imposed by the IDS-tests, the *I*-component quickly regenerated itself in all $K' < 1$ tests to the same magnitude as if $K' = 1$. In contrast, the *D*-component progressively increased its low-strain mobilization as K' decreased, and *D* remained greater at all IDS-test strains than if tested at $K' = 1$.

It appears that the very low rates of strain during secondary compression permitted the soil to change structure so as to increase its shear sensitivity to effective stress change. This increased sensitivity gradually diminished with increasing IDS-test strain.

9.4 COMPONENT TRANSFER DURING CREEP TESTS, NEGATIVE *I*

R. G. Bea (1960, 1963) performed a particularly interesting series of creep experiments on remolded, duplicate specimens of kaolinite and Boston blue clay. He subjected specimens to various levels of compressive loading and allowed them to creep under these constant loads. After various load and time intervals, and therefore accumulated strain, he subjected these specimens to constant-σ_1' IDS-tests. By comparing the *I*- and *D*-component distributions after creep with those distributions obtained from specimens compressed to the same strain, but without creep loading, he could evaluate the effect of creep on the component mobilization and distribution. *Fig. 24*, taken from Bea's thesis, presents the results he obtained from one series of tests on kaolinite. He obtained similar results from Boston blue clay, see Bea (1963).

Fig. 24 shows the component distributions found after three creep tests, compared with the component distributions from two duplicate tests on kaolinite specimens IDS-tested without prior creep. The IDS-tests started at the strains indicated by the light, dashed vertical lines. Also shown are the first *I* and *D* component points determined after a small additional strain during the subsequent IDS-test, as well as the subsequent variation of these components with continuing strain in that IDS-test. Clearly, as emphasized by the shading, the previous creep produced an abrupt increase in the *D*-component compared to that which otherwise would have been mobilized at that strain without creep. After creep, this kaolinite, and also the Boston blue clay, had greatly increased initial tangent moduli and a structure able to resist considerably greater compressive load than if the prior creep had not occurred. However, these increases in ability to mobilize shear resistance dissipated after about 1 to 2 % increase in axial strain during the IDS-test. Note that the above behavior seems quite consistent with that observed to result from the K' consolidation effects discussed in 9.3, and the secondary compression effects discussed in 9.2. All these behaviors seem to result from the same, or at least similar, soil structure phenomena.

R. G. Bea (1960) also showed that prior creep could produce an increase in the *D*-component to a level greater than the soil could mobilize without an interval of creep. *Fig. 25*, also taken from Bea's thesis, illustrates this phenomena. This Boston blue clay actually mobilized apparent effective stress friction angles, $\tan^{-1} d_\epsilon$, of 30 degrees while it can only mobilize about 24 degrees in an IDS-test strained much more rapidly to the same strain. Extrapolating to the 0-strain condition at the beginning of the IDS-test produces apparent friction angles as great as 33 to 34 degrees.

The question of the component distribution at the end of creep, corresponding to the 0 % strain during the subsequent IDS-test, of course has great interest. One can obtain estimates of such components by extrapolating the data obtained during subsequent strain by the IDS-test to the condition of 0 strain. A great deal of experience has shown that the *D*-component usually varies very gradually at low IDS-test strain while the *I*-component often increases very abruptly. Typically, the *I*-component has a very high modulus compared to the *D*-component. As also explained and illustrated by Schmertmann and

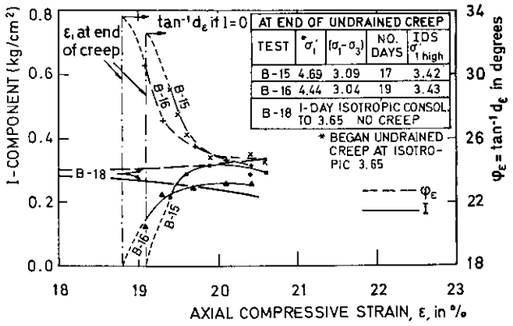

Fig. 25. Example of excess *D*-component mobilization after undrained creep in remolded Boston blue clay (from Bea 1960).

Hall (1961a), it therefore seemed logical to these authors to extrapolate the *D*-component to 0 strain and then compute the *I*-component that existed to provide the proper total of *I*- and *D*-components. After doing this, Schmertmann and Hall found a dramatic reduction in the *I*-component mobilized at the 0 IDS-test strain condition. The *I*-component dropped to near 0 in some cases and to –0.08 kg/cm² in one case.

The above negative value of *I* seemed impossible at the time and was attributed to experimental error. However, Bea obtained negative values that cannot be ignored when using similar, seemingly very logical, extrapolation procedures for the components at 0 strain. He reported negative values of 0-strain *I*-component in over half of his tests. For the remolded kaolinite he reported negative values ranging from –0.12 to –0.20 kg/cm², and for remolded Boston blue clay from –0.07 to –0.52 kg/cm². These 0-strain *I*-components did not correlate with the creep strain-rate just prior to the IDS-test. However, they did become increasingly negative with the incidental overconsolidation that occurred during creep in relation to the highest σ_1' used in the subsequent IDS-test (OCR = 1.6 @ above –.52).

9.5 COMMENTS ON TIME-TRANSFER EFFECTS

All of the above time effects indicate that during a period of constant loading, or very slowly increased loading, both involving very small time rate-of-strain, the structure of a soil readjusts in such way as to: 1) increase its reserve strength for subsequent small increases in strain, 2) this increase in strain is accompanied by an increase in shear modulus, and 3) these increases in shear resistance result almost entirely, and perhaps entirely, from an increase in the *D*-component.

Fig. 26 presents a quantitative illustration of this CSME behavior with pieces of CSMEs obtained from some of Bea's tests on remolded Boston blue clay, both with (1,2) and without (3,4) prior creep. Note the negative *I extrapolation* at the end of creep (the entire CSME still passes through $I_0 = 0.14$). Also, from comparison with the IDS-test results without creep one can see that this clay

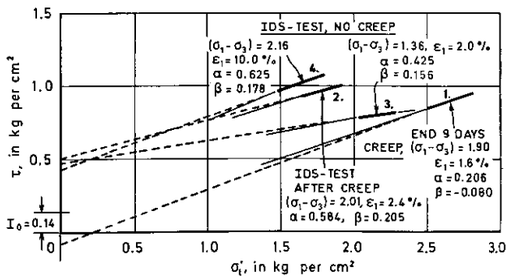

Fig. 26. Changes in the CSME with strain with and without prior creep in remolded Boston blue clay.

Table 16. The effect of creep on the *I* and *D* components in undisturbed BBC (stresses in kg/cm²).

Test	Creep		At end of creep			Without creep	
	$(\sigma_1-\sigma_3)$	Days	ε_1 (%)	$\tan^{-1} d\varepsilon$	*I*	$\tan^{-1} d\varepsilon$	*I*
B-13	2.02	11	2.50	15.0°	0.31	11.0°	0.51
B-14	2.00	3	2.00	15.1°	0.27	9.5°	0.54

increased its shear mobilization capability, and sensitivity d_ε, at $\varepsilon_1 = 2$ %, compared to had the creep to $\varepsilon_1 = 1.6$ % not occurred. It appears that the soil structure yields to those elements within the structure that have increased rigidity and also an increased sensitivity to a subsequent change in effective stress.

During strain-rest the passage of time allows the *I*-component to reduce dramatically and may even become negative. The previously established "fact" that only a part of the *I*-component can consist of true bond shear resistance (or true cohesion) clearly demonstrates that the yielding of the *I*-component cannot be explained simply by a time-reduction in some type of true cohesion behavior. Although Bjerrum's recent work (1973), as well as his work with T. C. Kenney (1968), showed a developing understanding of time-transfer from the less rigid to the more rigid shear resistance framework within a soil, Bjerrum attributed this to a relaxation of the true cohesion within the soil. The work presented herein seems to show clearly that any such true cohesion transfer can only account directly for a small portion of the *I*- to *D*-component transfer. If such small cohesion transfer does exist, it may, or it may not, indirectly trigger the particle behavior producing the major portion of this transfer.

The component time-transfer effects discussed thus far occurred in kaolinite and Boston blue clay first remolded by machine extrusion. Do they also occur in undisturbed clays? The work by Bjerrum and Wu (1960) and Bjerrum and Lo (1963) suggests that they do in at least some undisturbed Norwegian clays. As another example, Bea also tested undisturbed specimens from the same block sample of BBC that supplied the source for the extruded specimens.

Table 16 presents the results of Bea's constant-σ_1' IDS-tests on undisturbed BBC after undrained creep. It includes a comparison between the shear components at the end of creep and at the same strain in a similar IDS-test, but without prior creep.

Table 16 shows that *I* dropped about 45 % and d_ε increased about 33 % during creep.

It seems clear that the component time-transfer phenomena also occurs in at least some undisturbed cohesive soils. But Bea's experiments showed less transfer in undisturbed BBC, with its $I_{0m} = 0.27$ kg/cm², than in remolded BBC with $I_{0m} = 0.14$ kg/cm² (see "Undisturbed" in *Fig. 11d*). With all else equal perhaps stronger internal bonding between particles reduces the number and/or degree of soil structure adjustments that occur during creep to produce the *I* to *D* component transfer.

10. One explanation for the observed shear behavior

Over the span of this research the writer has devoted much thought to finding one or more hypotheses that might explain all the observed behavior in a logical, hopefully simple, manner consistent with the observations and with the particulate nature of soil. To date he can offer only the following for others to consider and improve upon.

10.1 THE CONSTANT *I*-COMPONENT DUE TO CONSTANT β

This remarkable constant-*I* behavior, as detailed in Section 4.1, may perhaps now be explainable – at least in a mathematical sense. Section 4.1 demonstrated that for a given soil, and a given effective stress, the *I*-component remained essentially the same no matter what was done to change the soil structure. *Fig. 27* illustrates two CSMEs for the same soil but at different structural conditions. In both cases I_0 represents only a minor fraction of the total *I*-component. In both cases, the IDS-piece-of-CSME, when extrapolated, produces the same *I*-component. Why? Start with the following equation (9) for *I*:

$$I = \tau - d_\varepsilon \sigma_t' \quad \ldots\ldots\ldots\ldots\ldots (9)$$

Substituting τ from Equation (6) into (9) produces the following equation (10):

$$I = I_0 + (\alpha - d_\varepsilon)\sigma_t' - \beta\sigma_t' ln\sigma_t' \quad \ldots\ldots\ldots (10)$$

After recognizing that $(I - I_0)/\sigma_t' = \beta$, Equation (10) rearranges to the following:

$$(\alpha - d_\varepsilon) = \beta(1 + ln\sigma_t') \quad \ldots\ldots\ldots\ldots (11)$$

As was shown in *Figs 11* and *12* herein, as well as some of the Section 7.4 example cases from undisturbed clays, the value of β at I_m seems remarkably independent of structure. Therefore, any two structural conditions 1 and 2 of the same soil in *Fig. 27* should have at least approximately the same value of β. A constant β despite a changing α produces a constant curvature and hence a constant difference between the α and d_ε slopes at any given σ_t'. In *Fig. 27* the writer used equation (6) to plot pieces of CSMEs around $\sigma_t' = 2.0$ using the same values of I_0 and β, but different α values to express the different soil structure. As must be true at any σ_t', the two values of $(\alpha - d_\varepsilon)$ at $\sigma_t' = 2.0$ are the same.

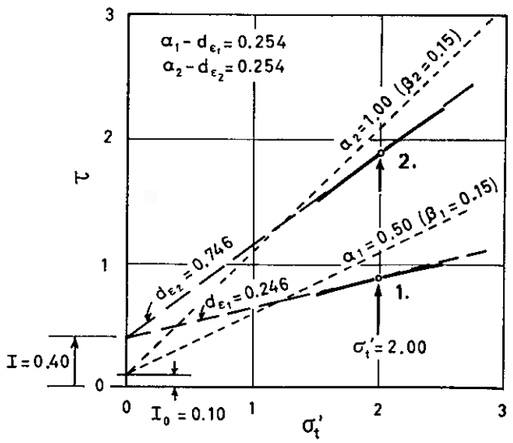

Fig. 27. Example illustrating *I* constant because $(\alpha - d_\varepsilon)$ constant.

Equation (10) shows a constant β and $(\alpha - d_\varepsilon)$ difference must result in the same *I*-component at a given σ_t', as also shown in *Fig. 27*. This holds provided I_0 does not change significantly with a change in structure or if I_0 is so small any significant change in I_0 has a negligible affect on the apparent constancy of the total *I*-component.

10.2 THE CONSTANT β AND GRAIN SIZE

This research has shown that β represents an approximate constant which expresses the curvature of the CSME. At or after the strain of I_m β does not vary with structure for a given soil during the forced rate-of-strain in an IDS-test, nor even very much in a particular class of soils. However, as noted in Section 5.1, β does appear to vary with grain size. After looking into this more carefully and plotting in *Fig. 28* the variation of I_m for various remolded soils as a function of the log of the D_{50} grain size, a remarkable fact emerges. Not only does I_m vary linearly with the level of effective stress, as explained previously in Section 5 in great detail, but I_m also varies inversely with log D_{50}. However, note the one exception to the general trend – the glass spheres have a much lower I_m than their size would indicate. In fact, I_m for glass spheres has proven consistently slightly negative (see *Tables 10, 14*).

From *Fig. 28* it appears clear that the value of β somehow depends on grain size. But, the zero or negative value of β for near-spherical glass particles shows that size alone is probably not the real criteria. The writer suggests that instead the curvature of the particles at contact controls β. It seems reasonable to postulate that the smaller the particles in contact, and therefore the more irregular and plate-shaped their geometries, then the smaller the average radii of curvature at the contact points. Because of the higher void ratios associated with finer particles, and their progressively less spherical geometries, a given effective stress produces progressively greater particle contact pressures as size decreases. This produces greater opportunity for local crushing, particle breaking, and any other nonlinear behavior, and thus progressively reduces effective stress sensitivity (slope) of the CSME with increasing σ_t'. Such a theory would show why the glass spheres do not fit with the other soils in *Fig. 28*. They have an almost spherical shape and therefore very high radii of contact relative to their size when compared to the rough, pitted and peaked surface of natural grains. Such a theory would also explain the constancy of β – the same or similar soil has the same or similar particles in contact, with statistically similar

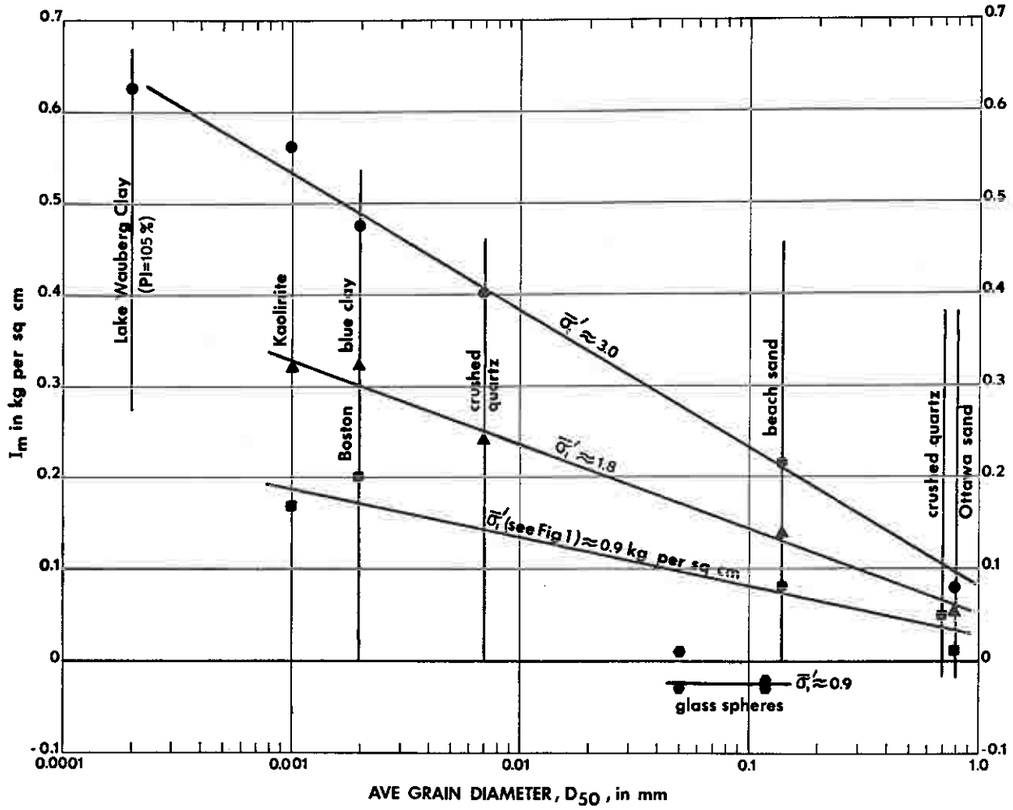

Fig. 28. The effect of grain size on I_m at constant effective stress.

average contact radii, regardless of their structural arrangement.

10.3 THE CONSISTENCY OF THE INCREASE IN *D*-COMPONENT WITH STRUCTURAL CHANGES

As detailed throughout this paper, and in marked contrast with the *I*-component, changes in soil structure have a dramatic effect on the strain-rate of mobilization of the *D*-component. Furthermore, the following treatments of a soil all seem to have the very similar effect of increasing the subsequent d_ε ($= \Delta\tau/\Delta\sigma_t'$):

1. A simple increase of strain at the same time rate-of-strain.
2. A decrease in the time rate of forced strain.
3. Allowing the soil to reach a creep-equilibrium (a very low rate-of-strain) under a constant deviator stress.
4. Allowing the soil to creep internally using increasing times for secondary compression with no deviator stress.
5. Subjecting the soil to overconsolidation.
6. Reducing the soil fluid viscosity while keeping rate-of-strain constant.

Clearly something very common in the behavior of soils must occur in these diverse treatments. In all we have the common element of either subjecting the soil structure to greater strain or allowing the structure to readjust during significant time periods of constant stress, or both. It seems that time and strain, or combinations, produce a structure readjustment that transfers load to the stronger, stiffer, but also more effective stress sensitive, groups of particles within the soil mass.

10.4 THE MYSTERIOUS *I*- TO *D*-COMPONENT TIME TRANSFER

Section 9.5 already summarized the possible significance of this component-transfer behavior. Once again: The bond shear resistance, I_0, usually, at least in these experiments on remolded soils, at ordinary effective stress levels represents a minor part of the total *I*-component. Also, in some circumstances after long periods of creep, the *I*-component can actually become negative. These observations seem to indicate clearly that the *I*-component represents only the extrapolated reflection of something else more fundamental happening within the soil structure.

The above 10.3 describes this more fundamental behavior, which involves a structure readjustment during the periods of relative strain-rest, which in turn produces a greater $\Delta\tau/\Delta\sigma_t'$ sensitivity at the same σ_t' level. Consequently, the extrapolation for the *I*-component produces a progressively reduction in *I*, even into negative values for soil structures still capable of developing enough additional $\Delta\tau/\Delta\sigma_t'$ sensitivity. *Fig. 26* illustrates this concept.

10.5 PARTICLE INTERFERENCE EFFECTS PRODUCE INCREASES IN $\Delta\tau/\Delta\sigma_t' = d_\varepsilon$ SENSITIVITY

Many of the clays tested in this research were first extruded mechanically into duplicate specimens by a "Vac-Aire" machine (described in Matlock et al., 1951). In this process an auger places successive smears of near-perpendicular-to-the-cylinder-axis, helical layers of clay as it simultaneously forces out an extruded cylinder of clay through a funnel mold. The samples used for the tests reported in *Table 17* had only a 7.9 to 7.6 cm mold diameter reduction and probably produced a fabric with a very strong preference for horizontal positions for the flaky particles. The triaxial specimens had a final mold reduction from 7.9 to 3.6 cm, probably producing some vertical fabric as a smear on the perimeter. Slow-dry shrinkage tests on triaxial specimens of DWEPK still showed a distinct preference for vertical volume change (65 % vs. 33 % if isotropic), and therefore presumably still a strong horizontal fabric preference. All extruded specimens would also have some degree of helical fabric superposed.

Despite the above extrusion remolding, these clays still had considerable strength sensitivity in subsequent laboratory vane shear tests. This sensitivity continued, and even increased, after the additional particle orientation by further chemical-induced dispersion, as discussed in 4.1.1. *Table 17* presents relevant data obtained after any post-extrusion thioxotropic changes had stopped, as monitored by changes in s_{uv}.

Note as perhaps expected, that s_{uv} and S_t both decrease when comparing the different dispersed kaolinites at the *same water content*. But, when *just above the PL*, s_{uv} remains about the same while S_t may actually increase!

Table 17. Vane shear sensitivity despite dispersion and extrusion of clays.

Soil (see Table 1)	Extruded water content (%)	*PL* (%)	s_{uv} (kg/cm²)	Vane S_t
DWEPK	42.5	31	0.22	2.2
	33	31	1.1	3.5
N-EPK	34	29	0.17	2.5
	31	29	0.7	3.8
Q-EPK	27	26	1.5	4.2
BBC	26.5	20	0.6	2.0

Table 18. Examples of pre-dispersion of soil structure increasing strain-rate of d_ε mobilization.

Extruded soil	Av. tan⁻¹ dε (degrees) at IDS-test axial compressive	
	$\varepsilon_1 = 1.0$ %	$\varepsilon_1 = 3.0$ %
Kaolinite (DW-EPK)	3.5	9
N*-EPK	5	11
Q*-EPK	10	19
Boston blue clay (BBC)	4	10
Q*-BBC	8	16

* Denotes addition of sodium phosphate dispersant prior to extrusion.

The explanation for the above perhaps surprising behavior may lie with the relation between particle and vane orientations. The lab vane, with height/diameter = 1.0, tests primarily (about 77 % in isotropic clay) the vertical plane. The ten complete revolutions prior to the remolded vane test probably forces particles to a more parallel orientation with the cylindrical failure surface, i.e. vertical. Because extrusion at lower water content, with or without the aid of dispersants, produces a progressively more horizontally dispersed particle orientation, the greater the interference of these particles with the forced reorientation by the vane. The greater this intereference, the greater the vane strength, s_{uv}, and also its percent reduction after the forced particle reorientation. Therefore we also had greater S_t despite greater dispersion.

Table 1 showed that the above dispersion, aided with chemicals, had little or no effect on the IDS-test I_m value. But, *Table 18* presents data that shows that such dispersion did increase dramatically the strain-rate of *D*-component mobilization. Why? As with the vane, the 45–60 degree (with the horizontal) most critical failure surface in compression tests forces considerable particle reorientation to align the near-horizontal particles with most-critical planes. The greater the degree of dispersion to horizontal particle positions, the greater the subsequent particle interference with this re-alignment process. Particle interference effects imply dilatent behavior, which is strongly effective stress dependent. Thus, the unfavorable particle orientations of dispersion, combined with the increased particle density after drained dispersion, produces the subsequent dramatic increase in the strain-rate of *D*-component mobilization.

Figs 7 and *8* illustrated the consistent observation that simple, isotropic overconsolidation would increase the strain-rate of a soil's *D*-component mobilization but not affect the *I*-component. *Fig. 23* illustrated that this increase in *D* was even more pronounced after anisotropic consolidation. Of course, isotropic overconsolidation forces a denser soil structure and anisotropic consolidation with $K' < 1$ adds some particle reorientation favoring the horizontal. Thus such prior consolidation would also add horizontal dispersion and increase particle interference effects and produce a subsequent strain-rate increase in *D* and $\Delta\tau/\Delta\sigma_t'$ sensitivity.

The writer has also observed on numerous occasions that the formation of a distinct failure plane in a specimen during an IDS-test would produce a relatively abrupt drop in I and a corresponding increase in d_ε. The last data point in *Fig. 5* shows such a drop in the I-component resulting from a failure plane developing just before the point. A failure plane represents a localized zone of very high shear strain. Very large strain disperses particles to a parallel orientation with the failure plan – as dramatized by slickensides. The sudden strain associated with the failure plane suddenly (with overall strain) increases the particle interference effects which resist the dispersion needed to form the plane. The effective stress dependency of such interference produces a sudden increase in d_ε, with a resultant drop in the I-component.

Considering the similarity of d_ε sensitivity effects produced by the structure effects of creep under external hydrostatic and/or deviator stresses, using pore fluids with reduced viscosity, or allowing much slower rates-of-strain, the writer believes that all of these treatments have the effect of changing particle orientations such that particle interference effects develop more rapidly with subsequent strain. But, one must also consider the matter of degree. For example the writer imagines that significant overconsolidation of a soil mass would produce a general reorientation throughout the mass and thus increase the D-component over a large interval of subsequent strain. But, particle reorientations involving less movements and strain, such as secondary compression and creep, would be more limited and the subsequent D-component increases would last for only limited subsequent strain. Also, using pore fluids with reduced viscosity would permit the particle interference effects to develop faster with strain because of less resistance to moving the pore fluid out of the way. The less the viscosity, the greater the d_ε mobilization, as in *Fig. 10.*

10.6 DIFFERENCE IN STRAIN-MOBILIZATION OF THE I- AND D-COMPONENTS

The many IDS-test experiments on remolded and undisturbed soils have all shown that the extrapolated I-component mobilizes at very low strain. For example, special low-strain IDS-tests on kaolinite, Enid and Boston blue clays show I_m at about $\varepsilon_1 = 0.2\,\%$. This probably represents mostly elastic strain involving only minor particle reorientations. In contrast, these clays require about 10–15 % strain for full d_ε mobilization – although progressively less with prior overconsolidation, secondary compression or creep. Initially (before 1963) the writer described this behavior as a rapid mobilization of the "cohesion" component vs. a slow mobilization of the "friction" component. Such description presents an oversimplified picture. The writer recommends instead the following more accurate description, although unfortunately also more complicated.

After a time interval of relative very slow rate-of-strain, as after creep, the soil structure will have just completed a period of drained dispersion. Particles in a favorable position to do so will have reoriented to more dispersed (lower potential energy) positions. Because the applied shear stress remains constant during this time, any loss of shear-carrying capacity due to reorientation by some particles must be taken up by those particles least likely to reorient. These are also the particles with the greatest interference effects. The immediate subsequent shear resistance obtainable under a newly forced increase in rate-of-strain now resides primarily in those particle groups with greater interference effects and therefore greater d_ε. Because the sum of the I- and D-components remains the same, a greater d_ε must cause a drop in the extrapolated I-component (see CSME 1 in *Fig. 26*).

The subsequent forced increase in rate-of-strain then produces an almost immediate, perhaps essentially elastic, mobilization of these relatively rigid maximum-particle-interference zones of shear resistance. As soon as interparticle movements again begin and β again controls CSME curvature, I increases to its curvature-controlled I_m (as at CSME 2 in *Fig. 26*). As the soil continues to strain it again mobilizes its ordinary particle-interference structure and not just the above rigid zones it was temporarily "leaning on". With this rigid-destruction to ordinary- mobilization transfer the value of d_ε, and therefore the D-component, rapidly diminishes during the very low increment of overall strain it takes to accomplish the transfer. d_ε then gradually increases again provided the soil structure has the capability of increasing its net particle interference effects with continued strain.

The above explanation would predict that a soil carrying a deviator stress under creep rate-of-strain conditions would have a high d_ε mobilization, and therefore a low extrapolated I-component. With the IDS-test forced increase in rate-of-strain, the I-component would rapidly rise and d_ε (and therefore the D-component) rapidly decrease with strain. Bea found exactly this behavior, as illustrated in *Figs 24, 25* and *26*. This behavior would not ordinarily be observed in an IDS-test beginning after isotropic consolidation because the mobilized D-component would begin at zero.

10.7 I_0 DRAINED VS. I_0 UNDRAINED

If I_0 represents the shear resistance of a soil due to its internal bonds between particles, then its mobilization must also be strain and possibly strain path dependent. As detailed in Section 5.2, K.-H. Ho did indeed prove that I_0, as well as P. Rowe's c_f, mobilized as functions of strain in at least some soils (each of 3 Ho investigated). I_0 might well also be anisotropic and stress and/or strain path dependent.

The data from Ho in *Table 14* seems to show that both I_0 and c_f values obtained from constant-volume (undrained) IDS-tests have a greater magnitude than when obtained from constant-σ_1' IDS-tests. It would seem that forcing a structure to strain at constant volume forces that structure to mobilize more of its internal bond shear resistance. Perhaps more interparticle movements per unit shear strain must occur at constant volume compared to when the soil structure can increase or decrease volume if free to do so.

Note also in *Table 14* that for the constant-volume tests c_f exceeds I_0 substantially. However, if c_f and I_0 were theoretically equivalent after a proper stress-dilatency correction to I_0, and remembering that the constant-volume ϱ-correction = 1.0, then these two parameters should be identical. That they are not perhaps indicates that the Rowe dilatency correction does not completely account for all soil-structure effects.

10.8 IMPLICATIONS FROM THE SUCCESS OF CURVE-HOPPING

The success of the one-specimen IDS-test curve-hopping technique demonstrated by Schmertmann (1962b) presents a puzzle which R. Kondner (1964) and Schmertmann (1964b) discussed. One might explain the success of curve-hopping by assuming the soil elastic over the effective stress range of the curve-hopping (usually approximately 20 % of initial effective stress). However, we know that soils do not behave elastically and especially not at strains beyond the initial high-modulus, low-strain portion of any type of soil shear test. Kondner rejected such an elastic explanation and the writer agrees.

What then can explain the success of curve-hopping? The only explanation the writer can imagine involves thinking of a soil mass as composed of a great many zones, or "cells" within the mass wherein most of its shear resistance resides. Such resistance-cells form, are destroyed and then perhaps subsequently reform with the continuing strain. All such cells depend primarily on an effective stress prestress for their shear resistance capability. The sudden decrease of ambient effective stress during a curve-hop from the higher to the lower effective stress level reduces this effective stress prestress level in many of these resistance cells to the point that they cannot sustain the same level of shear resistance and they fail. The many such failures within the IDS-test specimen results in the sudden drop in that soil's ability to mobilize shear resistance at the strain of the effective stress hop. *Fig. 29*, points 1–2 illustrate this drop. Then the IDS-test strain continues along 2–3 and new cells form and the soil resistance-cell system recovers from the failure effects of the previous abrupt effective stress reduction. With reapplication of the original ambient effective stress level the soil can again mobilize its initial magnitude of shear resistance along path 3–4.

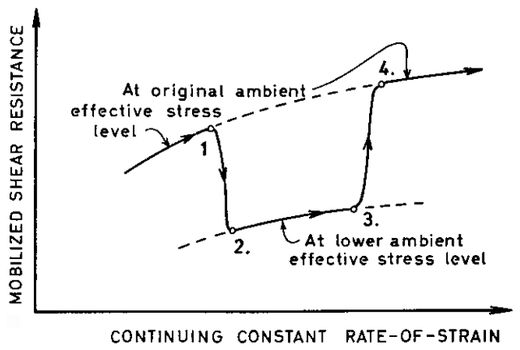

Fig. 29. A typical curve-hop in an IDS-test.

The *Fig. 29* path 1–2–3–4 ends at a point 4 seemingly no different , or not much different, than had the path been directly from 1 to 4 without the effective stress hop. The writer thinks the probable explanation for this superficially elastic behavior is that the number of cells progressively forming, collapsing and reforming with the continuing strain between points 1 and 4 is so large that the temporary, abrupt collapse of the cells during step 1–2 does not significantly change the overall resistance-cell system at the strain of 4. It appears to the writer that the overall mobilized shear resistance behavior of a soil structure represents the statistical summation of a very large number of formation-collapse events taking place within the structure. Any dislocation in the smooth flow of these events by a sudden effective stress change is only strain-temporary and is subsequently healed by the continuing many many events that take place with the continuing strain.

10.9 POSSIBLE NON-BONDING EXPLANATION OF "AGING" AND "QUASI-PRECONSOLIDATION"

When a soil can readjust its structure under drained conditions, such as during long periods of time at constant load, the more easily dispersed groups or zones of particles yield to those groups or zones of particles not easily dispersed. Such readjustment produces secondary compression in one-dimensional or isotropic consolidation, or creep if the soil can develop shear strain. With time the soil become stronger and stiffer as a result of this yield-transfer of mobilized shear. But, it also becomes relatively more effective stress sensitive (d_ε increases).

Any subsequent full mobilization of the shear capability of the new structure produces a yielding of the stiffer particle zones. After some interval of new strain to produce and exceed this yielding, with its accompanying many many resistance-cell events, the soil's mobilized shear resistance behavior returns to that which would have occurred had the drained dispersion interval not happened (as in *Fig. 9* at $\varepsilon_1 = 3\,\%$).

Such behavior would explain why soil "aging" and "quasi-preconsolidation" effects occur and possibly help evaluate when they would and would not occur. Clays are ordinarily the soils with the most complicated structure and the most subject to particle dispersion and reorientation effects. Such behavior is therefore potentially most important in clays. However, in principle it can also occur in sands and silts. From the work herein it would seem that it cannot occur when a structure has already been dispersed so that all particles have a minimum potential energy orientation. There would exist in such a structure (as on shear planes at the residual state)

no greater particle interference zones to temporarily "lean on".

The above has not introduced the possibility of additional interparticle bonds forming with time. Such would of course contribute to the "aging" and "quasi-preconsolidation" behavior. *Table 11* suggests that dispersion may increase such bonds. Cementing will also. However, the writer does not consider them essential to the phenomena.

10.10 COMMENT ON THE USE OF REMOLDED KAOLINITE VS. UNDISTURBED CLAYS

Because of the research need to compare tests while changing as few variables as possible, the writer made extensive use of tests from duplicate specimens remolded by machine extrusion – especially kaolinite. The reader might well wonder if the results obtained and the interpretations offered would apply to other clays – especially undisturbed clays?

As described and documented herein and in the references cited, several other extruded natural clays behaved the same as kaolinite with respect to IDS-tests, CSME curvature, component time transfer, etc. After satisfying himself on this point the writer then chose to use kaolinite more extensively, but not exclusively. It offered the advantages of availability in large quantities, ease of preparation and handling, a low secondary compression index, and the convenience of its relatively high permeability reducing the time required for pore pressure dissipation or equilibrium and making it easier to prepare saturated specimens. The interested reader can read Schmertmann (1963d) for more information about this kaolinite.

As also documented herein and elsewhere, the curve-hopping method and the IDS-test separation of components has proved possible in many undisturbed soils. Section 7.4 showed that the I vs. σ_t' method of extrapolation for I_0 seems to work as well in undisturbed as in remolded soils. Section 9.5 ended with data and discussion to support the idea that the component time-transfer behavior also occurs in undisturbed clays. All the available evidence the writer knows of supports the position that the various shear behavior phenomena investigated and described herein will occur in-situ in undisturbed clays. Of course one should expect great variations in degree.

11. Conclusions

A. *Relating to the constant structure Mohr Envelope (CSME)*

1. To achieve a more fundamental understanding of soil shear resistance behavior, one can investigate this behavior when keeping soil structure constant.
2. The concept and experimental use of the CSME provides a useful vehicle to explain constant-structure shear behavior.
3. This research has produced sufficient data to derive the following,

$$\tau = I_0 + \alpha\sigma_t' - \beta\sigma_t' ln\sigma_t' \quad \ldots\ldots\ldots\ldots (6)$$

expressing the shape of the CSME applicable to the soils and stress ranges investigated.

4. The β factor in the CSME equation seems to depend primarily on grain size and shape and probably reflects the nonlinear behavior occurring at particle contact points. The α factor seems to depend on soil structure.

B. *Relating to cohesion and the I-component*

5. The unexpected constancy of the I-component ("cohesion" intercept) with changes in structure results from the constancy of β and does not describe an invariable, fundamental shear component.
6. The I-component varies linearly with effective stress along the CSME because of the nature of CSME curvature.
7. One can determine a fundamental cohesion, or bond shear resistance, I_0, of any soil as a function of strain by new experimental methods described herein. The available alternate methods seem to check these I_0.
8. Typical remolded cohesive soils and natural, young, uncemented clays have maximum I_0 of about 0.05 to 0.15 kgf/cm^2. Cementing or partial saturation can greatly increase I_0. Drained structure dispersion probably increases the non-cementation part of I_0.
9. Because of CSME curvature, I_0 often represents only a minor part of the total I-component. Even sands with $I_0 = 0$ indicate a positive value for their I-components.
10. The strain-rate of I-component mobilization usually occurs much more rapidly than that of the D-component. But, the writer believes it premature to conclude from this alone that "cohesion" mobilizes quickly, while "friction" only gradually, with strain. The shape of the CSME can explain this behavior.
11. I_0 appears to mobilize at very low strain in cohesive soils compared to the strain required for overall soil failure. I_0 may, or may not, diminish greatly at overall failure.
12. Strain under undrained conditions appears to force a soil to mobilize more of its bond shear resistance than under drained conditions.

C. *Relating to the D-component and dispersion*

13. Deliberate chemical dispersion of structure, or overconsolidation, or increasing strain in a shear test, or increasing time in secondary compression, or increasing creep time under deviator loading, or decreasing a forced rate-of-strain, or using less viscous pore fluids all have the common effect of increasing a cohesive soil's subsequent shear resistance sensitivity to a change in effective stress.

14. The above 13. common effects suggest a common cause. The writer suggests that all the above manipulations produce an increased dispersion of soil structure, which leads to a transfer of a soil's shear resistance to those particles with greater resistance to dispersion.
15. After a period of time at constant loading, a soil becomes stronger and stiffer as a result of the continuing dispersion. The dispersion particle movements force the soil to "lean on" those groups of particles with greater resistance to dispersive reorientation. These groups have greater strength, greater stiffness, and – being brought nearer to failure – a greater sensitivity to changes in effective stress.

D. *Relating to "aging" behavior*

16. The above dispersion explanation for the increase in a soil's strength and stiffness with time may help explain soil "aging" and "quasi-preconsolidation" behavior.
17. One need not include the formation of new interparticle bonds to explain aging and quasi-preconsolidation behavior. Possibly, for the same reasons, one need not resort to the making and breaking of bonds to explain the undrained shear sensitivity of some soils.
18. Because of the more complicated soil structure possibilities in clays, they have a greater susceptibility to grain crushing/breaking and to dispersion and particle reorientation-interference effects. It seems reasonable to expect that the various shear resistance phenomena described herein would occur most dramatically in cohesive soils. However, in principle, one should also find such behavior as "aging" and "quasi-preconsolidation" in silts and sands.

E. *Some general thoughts from this work*

19. The overall behavior of a soil mass subject to strain at constant or increasing load represents the integration of effects from a huge number of resistance cell-formation and resistance cell-failure events that occur with changes in effective stress, strain and time.
20. The writer believes that d_ε ($= \tan\varphi_\varepsilon'$) represents a measure of a soil's mobilization of particle interference effects to resit applied shear. It appears that under constant-stress conditions a soil has more freedom to readjust its structure to more selectively, or at least more efficiently, mobilize its particle-interference strength against the next increment of applied shear than when subjected to a forced continuing strain, as in strain-controlled tests.
21. The maximum value of d_ε probably cannot be determined from a strain-controlled test. The value of d_ε will vary with the strain-time path used. Faster rates of forced strain will cause d_ε to decrease. Longer creep times will cause d_ε to increase.
22. The experiments described herein employed mostly remolded soils. However, all the present data indicate that the previous conclusions will also apply to soils in-situ.

List of notations

c_ε = early notation for I_ε.

c_t = P. Rowe's interparticle cohesion parameter, determined after using a stress-dilatancy correction. $\bar{c}_t$ = an average value.

CSE-test = experimental procedure for determining a constant structure envelope from a single specimen at one strain.

CFS-test = early notation for the IDS-test.

CSME = abbreviation for Constant Structure Mohr Envelope.

d_ε = alternate expression for the D-component, $= \Delta\tau/\Delta\sigma_t'$ (see Fig. 4).

D = component of mobilized shear resistance seemingly linearly dependent on effective stress, σ_t', at constant structure (see Fig. 4).

D_ε = notation for D to emphasize that component a function of strain.

D_{50} = that grain size in a soil with 50 % finer sized, by weight.

e = void ratio.

I = component of mobilized shear resistance seemingly independent of effective stress, σ_t', at constant structure. Note $I + D = \tau$. See Fig. 4.

I_ε = notation for I to emphasize that component a function of strain.

I_b = the maximum value of I_0 determined from a graph of I_0 vs. strain, the bond strength.

I_{df} = the value of I at a drained failure condition.

IDS-test = experimental procedure for determining the I and D components of τ as functions of strain.

I_m = the maximum value of I determined from a graph of I vs. strain.

I_0 = the mobilized shear resistance when $\sigma_t' = 0$, the bond shear resistance (see Fig. 13). $\bar{I}_0$ = an average value.

I_{0m} = the value of I_0 determined from an extrapolation of I_m to $\bar{\sigma}_t' = 0$.

I_{0u} = the value of I_0 determined from an extrapolation of I values at an undrained failure condition to $\bar{\sigma}_t' = 0$.

K' = the ratio of σ_3'/σ_1' at a point.

K_0' = the value of K' under conditions of no lateral strain.

n = porosity.

NC = abbreviation for normally consolidated.

NP = non plastic.

OC = abbreviation for overconsolidated.

OCR = overconsolidation ratio.

PI = Atterberg plasticity index.

PL = Atterberg plastic limit.

SL = shrinkage limit, by slow drying of extruded specimens.

s_{uv} = undrained shear strength determined by vane shear test.

S_t = sensitivity ratio of undisturbed to remolded undrained strength.

α = dimensionless soil structure parameter in equation (6).

β = dimensionless soil structure parameter in equation (6), $= \Delta I/\Delta\bar{\sigma}_t'$.

β_m = value of β when using I_m.

Δ = denotes "an increment of".

ε = strain.

ε_1 = major principal strain.

ε_{vol} = ε_v = volume strain.

ϱ = stress-dilatency correction factor, $= 1 + \Delta\varepsilon_v/\Delta\varepsilon_1$.

σ' = effective stress.

σ_1' = major principal effective stress, $\bar{\sigma}_1'$ denotes average value (see Fig. 4).

σ_2' = intermediate principal effective stress.

σ_3' = minor principal effective stress.

$\sigma_{1\,high}'$ = $\sigma_{1\,h}'$ = higher effective stress level in an IDS-test.

$\sigma_{1\,low}'$ = $\sigma_{1\,l}'$ = lower effective stress level in an IDS-test.

σ_a' = effective stress tension resistance.

σ_c' = hydrostatic effective stress from laboratory consolidation.

σ_m' = mean normal effective stress, $= \sigma_{oct}'$.

σ_{oct}' = octahedral normal stress, $= (\sigma_1'+\sigma_2'+\sigma_3')/3$.

σ_t' = normal effective stress on plane of CSME tangency, $\bar{\sigma}_t'$ = an average value of σ_t' (see Fig. 4).

τ = mobilized shear stress.

φ' = effective stress soil friction angle.

φ_e = early notation for D-component, $= \tan^{-1} d_e$.

List of references

Bea, R. G. (1960): *An experimental study of cohesion and friction during creep in saturated clay*. Master's thesis to the University of Florida, 107 pp., published in part by Bea (1963).

Bea, R. G. (1963): *Discussion on: Wu, T. H., A. G. Douglas and R. D. Goughmour: Friction and cohesion of saturated clays*. A summary of Bea (1960). American Society of Civil Engineers, Journal of the Soil Mechanics and Foundations Division, Vol. 89, No. SM1, pp. 268–277.

Bishop, A. W. and V. K. Garga (1969): *Drained tension tests on London clay*. Geotechnique, Vol. XIX, No. 2, pp. 309–313.

Bjerrum, L. (1973): *Problems of soil mechanics and construction on soft clays*. State-of-the-art-paper to Session IV, 8th I.C.S.M. & F.E., Moscow, Vol. 3, pp. 111–159.

Bjerrum, L. and T. C. Kenney (1968): *Effect of structure on the shear behavior of normally consolidated quick clays:* Proceedings of the Geotechnical Conference, Oslo, Vol. II, pp. 19–27.

Bjerrum L. and K. Y. Lo (1963): *Effect of aging on the shear strength properties of a normally consolidated clay*. Geotechnique, Vol. XIII, No. 2, pp. 147–57. Also publ. in Norwegian Geotechnical Institute Publication No. 57.

Bjerrum, L. and T.-H. Wu (1960): *Fundamental shear strength properties of Lilla Edet clay*. Geotechnique, Vol. 10, No. 3, p. 107, p. 108. Also publ. in Norwegian Geotechnical Institute Publication No. 38.

Crawford, C. W. (1963): *Cohesion in an Undisturbed Sensitive Clay*. Geotechnique, Vol. XIII, No. 2, p. 134, Fig. 1.

De Beer, E. E. (1965): *Influence of the mean normal stress on the shearing strength of sand*. 6th I.C.S.M. & F.E., Montreal, Vol. 1, p. 165.

Hansen, J. Brinch (1967): *Some empirical formulae for the shear strength of Molsand*. Proceedings of the Geotechnical Conference, Oslo, Vol. 1, pp. 175–177.

Ho, K.-H. (1971): *Theoretical and experimental relationships between stress dilatency and IDS strength components*. Dissertation to the University of Florida, 229 pp., unpublished.

Jakobson, B. (1953): *"Origin cohesion" of clay*. Proceedings 3rd I.C.S.M. & F.E., Zurich, Vol. 1, pp. 35–37.

Kondner, R. L. (1964): *Discussion on: Schmertmann, J. H.,: Generalizing and measuring the Hvorslev effective components of shear resistance*. American Society for Testing and Materials, Special Technical Publication 361, pp. 158–160.

Ladd, C. C. and T. W. Lambe (1963): *The strength of 'undisturbed' clay determined from undrained tests*. American Society for Testing and Materials, Special Technical Publication 361, p. 342 (also see M.I.T. preprint P-63–21, July, 1963 for a more accurate plotting of data).

Lambe, T. W. (1953): *The Structure of Inorganic Soil*. American Society of Civil Engineers, Proceedings, Vol. 79, Separate No. 315.

Leonards, G. A. and B. K. Ramiah (1960): *Time effects in the consolidation of clays*. American Soc. for Testing Materials, Special Tech. Publ. 254, pp. 116–130.

Matlock, H., C. W. Fenske and R. F. Dawson (1951): *De-aired, extruded soil specimens for research and for evaluation of test procedures*. American Society for Testing and Materials, Bulletin 177, October, pp. 51–55.

Mitchell, J. K. (1976): *Fundamentals of soil behavior*. John Wiley & Sons, New York.

Noorany, I. and H. B. Seed (1965): *In-situ strength characteristics of soft clays*. American Society of Civil Engineers, Journal of the Soil Mechanics and Foundations Division, Vol. 91, No. SM2, Part 1, pp. 49–80.

Rowe, P. W. (1957): $c_e = 0$ *hypothesis for normally loaded clays at equilibrium*. 4th I.C.S.M. & F. E., London, Vol. 1, p. 189.

Rowe, P. W. (1962): *The stress-dilatancy relation for static equilibrium of an assembly of particles in contact*. Proceedings of the Royal Society, A, Vol. 269, pp. 500–527.

Rowe, P. W., D. B. Oates and N. A. Skermer (1964): *The stress dilatancy performance of two clays*. American Society for Testing and Materials, Special Technical Publication 361, pp. 134–143.

Schmertmann, J. H. (1962a): *An experimental study of the development of cohesion and friction with axial strain in saturated cohesive soils*. Dissertation to Northwestern University, June, 116 pp.

Schmertmann, J. H. (1962b): *Comparisons of one and two-specimen CFS tests*. American Society of Civil Engineers, Journal of the Soil Mechanics and Foundations Division, Vol. 88, No. SM6, pp. 169–205.

Schmertmann, J. H. (1963a): *Discussion on: Wu, T. H., A. G. Douglas and R. D. Goughnour: Friction and cohesion of saturated clays*. American Society of Civil Engineers, Journal of the Soil Mechanics and Foundations Division, Vol. 89, No. SM1, pp. 260–268.

Schmertmann, J. H. (1963b): *Laboratory and computer study of a series of direct shear tests on sand*. Norwegian Geotechnical Institute internal report F.202.9, July 25., unpublished.

Schmertmann, J. H. (1963c): *Study of the reconsolidation behavior of Manglerud quick clay by means of constant-volume IDS-tests*. Norwegian Geotechnical Institute internal report F.234–1, unpublished.

Schmertmann, J. H. (1963d): *Discussion on: O'Neil, H. M.: Direct-shear test for effective-strength parameters*. American Society of Civil Engineers, Journal of the Soil Mechanics and Foundations Division, Vol. 89, No. SM3, Part 1, pp. 159–161.

Schmertmann, J. H. (1964a): *Generalizing and measuring the Hvorslev effective components of shear resistance*. American Society for Testing and Materials. Symposium on laboratory shear testing of soils. ASTM Special Technical Publication 361, pp. 147–162.

Schmertmann, J. H. (1964b): *Closure to discussion on: Generalizing and measuring the Hvorslev effective components of shear resistance*. American Society for Testing and Materials, Special Technical Publication 361, pp. 160–162.

Schmertmann, J. H. (1965a): *Discussion on: Crawford, C. B.: Interpretation of the consolidation test*. American Society of Civil Engineers, Journal of the Soil Mechanics and Foundations Division, Vol. 91, No. SM2, Part 1, pp. 131–135.

Schmertmann, J. H. (1965b): *Discussion on: Noorany, I. and H. B. Seed: In-situ strength characteristics of soft clays*. American Society of Civil Engineers, Journal of the Soil Mechanics and Foundations Division, Vol. 91, No. SM6, Part 1, pp. 123–127.

Schmertmann, J. H. (1972): *Hydraulic fracturing to determine K_0' and tensile strength*. National Research Council of Canada, Division of Building Research, Geotechnical Section, internal report on project G-1, unpublished.

Schmertmann, J. H. and J. R. Hall, Jr. (1961a): *Cohesion after non-hydrostatic consolidation*. American Society of Civil Engineers, Transactions, Vol. 128, Part I, pp. 949–981. Also publ. in A.S.C.E. as Proceedings Paper 2881, Journal of the Soil Mechanics and Foundations Division, Aug., 1961.

Schmertmann, J. H. and J. R. Hall, Jr. (1962): *Closure to discussion on: Cohesion after non-hydrostatic consolidation*. American Society of Civil Engineers, Journal of the Soil Mechanics and Foundations Division, Vol. 88, SM4, pp. 163–167. Also in Schmertmann and Hall (1961), pp. 976–981.

Schmertmann, J. H. and J. O. Osterberg (1961b): *An experimental study of the development of cohesion and friction with axial strain in saturated cohesive soils*. American Society of Civil Engineers. Research Conference on Shear Strength of Cohesive Soils, Boulder, Colo., pp. 643–694.

Strømann, H. (1971): *Laboratory test techniques for determining the constant-structure envelope of soils*. Master's thesis to the University of Florida, 135 pp., unpublished.

Topshøj, A.-G. (1970): *Bond strength of extruded kaolinite by triaxial extension testing*. Master's thesis to the University of Florida, 84 pp., unpublished.

Acknowledgements

As noted throughout the paper, the writer owes much to the work of the following students at the University of Florida (U. of F.): R. Bea, J. Hall, Jr., K.-H. Ho, H. Strømann and A. Topshøj. Their careful experimental work added greatly to the scope and quality of this study. U. of F. Engineering Technician W. Whitehead provided important support to the last three students listed.

Professors R. W. Kluge, former Chairman of the U. of F. Department of Civil Engineering, J. O. Osterberg, the writer's dissertation advisor at Northwestern University, and F. E. Richart, Jr., formerly in charge of geotechnical engineering at the U. of F., played an important part in the critical early stages of this work by making it possible for the writer to devote extensive time to the research during the years 1958–62. The writer also received important personal encouragement and advice from Drs. A. Casagrande, J. Hvorslev and K. Terzaghi. Special acknowledgement, as noted in the Introduction, goes to Dr. L. Bjerrum who through many personal and written debates helped the writer decide the scope and clarify the significance of this experimental work.

An important acknowledgement must go to those who made this work possible financially. The National Science Foundation, Engineering Mechanics Division, generously provided the bulk of the support through three research grants over the years 1958–71, as well as a Jr. Post-doctoral Fellowship for study with Dr. Bjerrum during 1962–3. The U. of F. Engineering and Industrial Experiment Station supplied critical funds for equipment during the early phases of the work.

Table of Contents

1. *Introduction* 65

2. *The constant structure Mohr envelope (CSME)* 65

3. *The IDS-test* 66
   - 3.1 Generalizing the Hvorslev components 66
   - 3.2 Test development to the use of a single specimen 67
   - 3.3 Variety of IDS-tests 68

4. *The constant I-component* 68
   - 4.1 The constancy of I_m 69
     - 4.1.1 Particle dispersion 69
     - 4.1.2 Void ratio and overconsolidation 69
     - 4.1.3 Simple overconsolidation 69
     - 4.1.4 Primary and secondary consolidation time effects 69
     - 4.1.5 Anisotropic consolidation 71
     - 4.1.6 Clay mineralogy and grain size 72
     - 4.1.7 Rate-of-strain effect 72
     - 4.1.8 Type of pore fluid 73
   - 4.2 I_m not cohesion 73

5. *I-component linear with effective stress* 74
   - 5.1 Considering I_m 74
   - 5.2 Considering I at any strain 75

6. *The shape of the CSME* 76
   - 6.1 The shape equation 76
   - 6.2 Independent experimental checks of CSME shape 77
     - 6.2.1 de Beer Tests 77

6.2.2 IDS-tests using different $\Delta\sigma_1'$ curve-hopping levels 77
6.2.3 Direct, single-specimen determination of the CSME 78
6.3 Conclusion regarding shape 78

7. *Determining the bond shear resistance from the CSME* 78
7.1 Definitions 78
7.2 The CSE-test method 79
7.3 The IDS-test method 79
7.4 Using the IDS-test method on undisturbed soils 80
7.4.1 Partially saturated quartz silt 80
7.4.2 A natural cemented sand 80
7.4.3 Undisturbed Norwegian quick clay 81
7.4.4 Two normally consolidated clays tested by "perfect samling" IDS-tests 81
7.5 An approximate, one specimen method 82

8. *Comparing I_0 with other methods* 83
8.1 Jakobson's origin cohesion 83
8.2 Tension tests 83
8.3 Rowe's stress-dilatency method 84
8.4 Conclusions on comparisons with other methods 85

9. *Time-transfer of IDS-components* 86
9.1 Rate-of-strain effects 86
9.2 Primary and secondary consolidation time effects 86
9.3 Effects during anisotropic consolidation 86
9.4 Component transfer during creep tests, Negative I! 87
9.5 Comments on time-transfer effects 88

10. *One explanation for the observed shear behavior* .. 89
10.1 The constant I-component due to constant β .. 89
10.2 The constant β and grain size 89
10.3 The consistency of the increase in D-component with structural changes 90
10.4 The mysterious I- to D-component time transfer 90
10.5 Particle interference effects produce increases in $\Delta\tau/\Delta\sigma_t' = d_s$ sensitivity 91
10.6 Difference in strain-mobilization of the I- and D-components 92
10.7 I_0 drained vs. I_0 undrained 92
10.8 Implications from the success of curve-hopping 93
10.9 Possible non-bonding explanation of "aging" and "quasi-preconsolidation" 93
10.10 Comment on the use of remolded kaolinite vs. undisturbed clays 94

11. *Conclusions* 94
A. Relating to CSME 1 thru 4 94
B. Relating to cohesion 5 thru 12 94
C. Relating to D-component and dispersion 13 thru 15 94
D. Relating to "aging behavior" 16 thru 18 95
E. Some general thoughts from this work 19 thru 22 95

List of notations 95

List of references 96

Acknowledgements 97